HHS Public Access

Author manuscript

J Comp Neurol. Author manuscript; available in PMC 2018 June 01.

Published in final edited form as:

J Comp Neurol. 2017 June 01; 525(8): 2000–2018. doi:10.1002/cne.24187.

A central mesencephalic reticular formation projection to medial rectus motoneurons supplying singly and multiply innervated extraocular muscle fibers

Martin O. Bohlen[1,*], **Susan Warren**[2], and **Paul J. May**[2,3,4]

[1]Program in Neuroscience, University of Mississippi Medical Center, Jackson, Mississippi

[2]Department of Neurobiology & Anatomical Sciences, University of Mississippi Medical Center, Jackson, Mississippi

[3]Department of Ophthalmology, University of Mississippi Medical Center, Jackson, Mississippi

[4]Department of Neurology, University of Mississippi Medical Center, Jackson, Mississippi

Abstract

We recently demonstrated a bilateral projection to the supraoculomotor area from the central mesencephalic reticular formation (cMRF), a region implicated in horizontal gaze changes. C-group motoneurons, which supply multiply innervated fibers in the medial rectus muscle, are located within the primate supraoculomotor area, but their inputs and function are poorly understood. Here, we tested whether C-group motoneurons in *Macaca fascicularis* monkeys receive a direct cMRF input by injecting this portion of the reticular formation with anterograde tracers in combination with injection of retrograde tracer into the medial rectus muscle. The results indicate that the cMRF provides a dense, bilateral projection to the region of the medial rectus C-group motoneurons. Numerous close associations between labeled terminals and each multiply innervated fiber motoneuron were present. Within the oculomotor nucleus, a much sparser ipsilateral projection onto some of the A- and B-group medial rectus motoneurons that supply singly innervated fibers was observed. Ultrastructural analysis demonstrated a direct synaptic linkage between anterogradely labeled reticular terminals and retrogradely labeled medial rectus motoneurons in all three groups. These findings reinforce the notion that the cMRF is a critical hub for oculomotility by proving that it contains premotor neurons supplying horizontal extraocular muscle motoneurons. The differences between the cMRF input patterns for C-group versus A- and B-group motoneurons suggest the C-group motoneurons serve a different oculomotor role than the others. The similar patterns of cMRF input to C-group motoneurons and

Correspondence: Paul J. May, Department of Neurobiology & Anatomical Sciences, University of Mississippi Medical Center, 2500 North State Street, Jackson, MS 39216., pmay@umc.edu.

*Present address: Martin O. Bohlen, Biomedical Engineering, 1427 CIEMAS, Box 90281, 101 Science Drive, Duke University, Durham, NC 27708-0281

CONFLICT OF INTEREST

The authors have no conflicts of interest to disclose.

AUTHOR CONTRIBUTIONS

All authors had full and open access to all the data in the study and take responsibility for the integrity of the data and the accuracy of the data analysis. Study concept and design: M.O.B. and P.J.M. Acquisition of data: M.O.B., S.W., and P.J.M. Analysis and interpretation of the data: M.O.B., S.W., and P.J.M. Drafting the manuscript: M.O.B. Critical revision of the manuscript for important intellectual content: M.O.B., S.W., and P.J.M. Obtaining funding: P.J.M. and S. W. Study supervision: S.W. and P.J.M.

preganglionic Edinger-Westphal motoneurons suggest that medial rectus C-group motoneurons may play a role in accommodation-related vergence.

Keywords

eye movement; oculomotor; primate (RRID: NCBITaxon:9541); vergence

1 | INTRODUCTION

It has long been recognized that extraocular muscle fibers can receive one of two types of innervation (Mayr, Gottschall, Gruber, & Neuhuber, 1975; Morgan & Proske, 1984; Schiaffino & Reggiani, 2011; Spencer & Porter, 1981, 2006). Approximately 80–90% of extraocular muscle fibers receive a single, *en-plaque* neuromuscular junction within the middle third of the muscle from large, heavily myelinated axons (Büttner-Ennever, Horn, Scherberger, & D'Ascanio, 2001; Namba, Nakamura, & Grob, 1968a; Namba, Nakamura, Takahashi, & Grob, 1968b). These are commonly referred to as "singly innervated fibers" (SIFs). Excitation of SIFs results in an all-or-nothing "twitch" response and, based on histochemical and ultrastructural features, their contraction characteristics are presumed to range from fatigable to fatigue resistant (Bach-y-Rita and Ito, 1966; Bach-y-Rita, Lennerstrand, Alvarado, Nichols, & McHolm, 1977; Bondi & Chiarandini, 1983; Chiarandini & Stefani, 1979; Jacoby, Chiarandini, & Stefani, 1989; Lynch, Frueh, & Williams, 1994; Nelson, Goldberg, & McClung, 1986). The other 10–20% of extraocular muscle fibers [Human: (Wasicky, Horn, & Büttner-Ennever, 2000) Rat: (Eberhorn, Büttner-Ennever, & Horn, 2006; Mayr, 1971)] are innervated by thin axons, which form multiple boutonal and *en-grappe* neuromuscular junctions along the entire length of the muscle fiber (Namba et al., 1968a, 1968b). These are commonly referred to as "multiply innervated fibers" (MIFs). MIFs have slow, graded, "non-twitch" responses (Chiarandini & Davidowitz, 1979; Chiarandini & Stefani, 1979; Jacoby et al., 1989; Nelson et al., 1986) and are categorized as highly fatigue resistant (Bach-y-Rita & Ito, 1966; Bach-y-Rita et al., 1977; Bondi & Chiarandini, 1983).

Medial rectus motoneurons are grouped into three distinct motoneuronal pools in monkeys, which were defined as the A-, B-, and C-group in early anatomical investigations (Büttner-Ennever & Akert, 1981; Porter, Guthrie, & Sparks, 1983). The A- and B-groups are found ventrolaterally and dorsocaudally, respectively, within the oculomotor nucleus (III), while the C-group is located within the supraoculomotor area (SOA), on the dorsomedial periphery of III. Büttner-Ennever et al. (2001) compared labeling from injections of the distal and central parts of the medial rectus muscle, reasoning that distal injections would just label MIF motoneurons. They concluded that the C-group supplied input to the MIFs, while the A- and B-group motoneurons supplied SIFs. Further studies showed that separate SIF and MIF motoneuronal pools are a general feature of each extraocular muscle in monkeys, with SIF motoneurons located within their respective nucleus, while MIF motoneurons found peripheral to their respective nucleus (Wasicky et al., 2004).

To date, we have limited understanding of the function of MIFs because their motoneurons have not been specifically recorded from during oculomotor behaviors. There have been investigations of MIF motoneuron inputs, in order to gain insight into their function. Wasicky et al. (2004) noted that anterograde tracers placed in the medial vestibular nucleus, Y group, and pretectum labeled terminals over the regions occupied by MIF motoneurons. More recently, retrograde trans-synaptic labeling experiments using rabies virus injections into the distal lateral rectus muscle of monkeys have identified MIF premotor neurons within the medial vestibular nucleus and the nucleus prepositus, the SOA and in the central mesencephalic reticular formation (cMRF) (Ugolini et al., 2006). With respect to the cMRF input, we recently noted that this region provides a considerable projection to the SOA in monkeys, and that the terminal field is particularly dense, immediately dorsal to III, where the C-group is located (Bohlen, Warren, & May, 2016). These results suggest that the cMRF may have direct projections to motoneurons involved in eye movement, and more specifically medial rectus MIF motoneurons.

Anatomically, the cMRF is a box-shaped region within the core of the caudal mesencephalon (Chen & May, 2000; Cohen, Matsuo, Fradin, & Raphan, 1985). With regards to connectivity, the cMRF projects to virtually all the brainstem regions associated with gaze changes [Monkey: (Cowie, Smith, & Robinson, 1994; Langer & Kaneko, 1990; Perkins, Warren, & May, 2009; Robinson, Phillips, & Fuchs, 1994; Wang, Perkins, Zhou, Warren, & May, 2013; Warren, Waitzman, & May, 2008); Cat: (Edwards, 1975; Edwards & de Olmos,1976; Langer & Kaneko, 1984; Perkins, May, & Warren, 2014)]. Arguably, the largest cMRF projection is to the superior colliculus [*Monkey*: (Chen & May, 2000; Wang et al., 2013; Zhou, Warren, & May, 2008); *Cat*: (Appell & Behan, 1990; Edwards & de Olmos, 1976)]. In turn, the superior colliculus provides a major input to the cMRF [*Monkey*: (Cohen & Büttner-Ennever, 1984; Harting, 1977); *Cat*: (Edwards, 1975; Perkins et al., 2014)]. As crossed tectobulbospinal tract axons exit the deep layers of the superior colliculus, destined for the contralateral predorsal bundle, they provide collaterals to the ipsilateral cMRF, before decussating on their way to the pons and medulla [*Monkey*: (Moschovakis, Karabelas, & Highstein, 1988); *Cat*: (Grantyn & Grantyn, 1982)]. So in addition to supplying the colliculus with input, the cMRF is privy to the target error signals sent from deep layers of the colliculus to the rest of the brainstem (Chen & May, 2000; Wang et al., 2013). In fact, stimulation of the monkey cMRF results in horizontal, conjugate, saccadic eye movements directed away from the stimulated side (Bender & Shanzer, 1964; Cohen et al., 1985; Cohen, Waitzman, Büttner-Ennever, & Matsuo, 1986). Furthermore, single cell recordings in head-fixed monkeys have revealed that cMRF neurons fire maximally for horizontal eye movements away from the recorded side (Cromer & Waitzman, 2006, 2007; Waitzman, Silakov, & Cohen, 1996). The specificity for horizontal eye movements was questioned by Handel and Glimcher (1997), but Waitzman and colleagues (2000a, 2000b) suggested that vertical gaze changes are controlled by the mesencephalic reticular formation rostral to the cMRF. This region has been termed the peri-interstitial mesencephalic reticular formation (piMRF) for its proximity to the interstitial nucleus of Cajal (InC).

In light of the cMRF's role in horizontal eye movements, a projection to medial rectus motoneurons seems reasonable. Indeed, transsynaptic retrograde experiments in the guinea pig indicate their midbrain reticular formation contains premotor neurons supplying the

medial rectus muscle (Graf, Gerrits, Yatim-Dhiba, & Ugolini, 2002). Furthermore, the cMRF's projection to SOA (Bohlen et al., 2016) suggests that it may specifically target C-group motoneurons. However, it is noteworthy that studies of the activity of cMRF neurons indicate that they fire a burst of action potentials for saccadic eye movements (Cromer & Waitzman, 2006; Moschovakis et al., 1988; Waitzman et al., 1996, 2008), in contrast to the other regions thought to supply input to MIF motoneurons (e.g., medial vestibular nucleus, nucleus prepositus, and SOA). These non-cMRF inputs primarily supply motoneurons with tonic signals that are appropriate for the expected slow, graded nature of MIF contraction, which may be useful for maintaining eye position. Thus, it seemed reasonable to test whether the cMRF projects directly to medial rectus motoneurons in primates, and to determine whether it specifically contacts the MIF motoneurons within the C-group. To examine these possibilities in *M. fascicularis* monkeys, we employed dual tracing techniques in which an injection of retrograde tracer was made into the medial rectus muscle to label all three subgroups and an anterograde tracer was placed in the cMRF to label terminals in and around the oculomotor nucleus. Due to the fact that the cMRF's SOA projection was bilateral (Bohlen et al., 2016), in separate animals, we utilized muscle injections ipsilateral and contralateral to the side of the cMRF injection. Portions of this work have appeared in abstract form (Bohlen, Warren, & May, 2015; May, Horn, Mustari, & Warren, 2011).

2 | METHODS AND MATERIALS

These experiments were performed using seven adult or young adult *Macaca fascicularis* monkeys (RRID: NCBITaxon:9541) of both sexes. The methods described are in accordance with NIH guidelines for animal care and use, and were approved by the University of Mississippi Medical Center's IACUC. Animals were sedated with ketamine hydrochloride (10 mg/kg, IM), administered with atropine sulfate (0.05 mg/kg, IM) to reduce airway secretions. They were then intubated and anesthetized on a 1–3% isoflurane/oxygen mix for the duration of the surgery. Temperature, heart rate, and rate of respiration were continually monitored and maintained within physiological norms. Each animal also received Carprofen (3 mg/kg, IM) as a preemptive analgesic. After closing, Sensorcaine (0.5–1.0 ml) was administered at the incision site. Buprenex (0.01 mg/kg, IM) served as a postsurgical analgesic.

Once anesthetized, animals were placed into a stereotaxic apparatus (Kopf Instruments, Tujunga, CA). The approach for central injections into the cMRF has been described elsewhere in detail (see Bohlen et al., 2016; May, Warren, Bohlen, Barnerssoi, & Horn, 2016) and will be briefly described here. Medial parietal cortex was aspirated to visualize the superior colliculus and caudal pole of the pulvinar. Antero-grade tracer injections were stereotaxically placed into the cMRF with the aid of a primate stereotaxic atlas (Szabo & Cowan, 1984). A 1 μl Hamilton microsyringe containing 10% biotinylated dextran amine (10,000 MW) (BDA; n =6; Invitrogen) or a glass micropipette containing 2% *Phaseolus vulgaris* leucoagglutinin (PhaL; n =1; Vector Laboratories Cat# BA-0224, RRID: AB_231544) was held in a micromanipulator that was angled 10 °, tip rostral in the sagittal plane, and then rotated 10–11° clockwise, when observed from above. The needle or micro-pipette was inserted through the pulvinar and lowered to a point ~7 mm below the surface of the superior colliculus. Along each track, two, 0.1 μl pressure injections of 10% BDA were

made approximately 1 mm apart. In some cases, a second track was made with the needle inserted at a different mediolateral position. For PhaL injections, the tracer was dissolved in pH 8.0, 0.1 M phosphate buffer (PB). Injections were made from a glass micropipette with a 20 μm tip by iontophoresis (Model CS 3; Transkinetics; Canton, MA), using 7 μA, 7 s, square wave pulses for 10 min at each injection site (see Wang et al., 2013 for details). At the end of the surgery, incised tissues were sutured back together.

A second peripheral surgery was performed 14–20 days later to inject a retrograde tracer into the medial rectus muscle. The general surgical and anesthetic procedures were the same as for the first injection. An incision was made along the supraorbital ridge and then the orbicularis oculi muscle was disinserted to reveal the orbital contents. The medial rectus muscle was isolated and injected with 7 μl of 2% wheat germ agglutinin conjugated to horseradish peroxidase (WGA-HRP) or choleratoxin B subunit conjugated to horseradish peroxidase (ChTB-HRP) with a 10 μl Hamilton syringe (n =7; four muscles ipsilateral to the injected cMRF; three muscles contralateral to the injected cMRF). Tracer was placed in both the belly and the distal end of the muscle at the insertion. The orbicularis oculi muscle was reattached and the incision site was closed with suture.

Two days after the muscle injection, animals were sedated with ketamine HCl, and then deeply anesthetized with sodium pentobarbital (50 mg/kg, IP). They were then transcardially perfused with 0.1 M, pH 7.2 phosphate buffered saline, followed by 3 L of a mixture of 1% paraformaldehyde and 1.5% glutaraldehyde in 0.1 M, pH 7.2 PB. The brainstem was blocked in situ in the frontal plane. It was then postfixed in the same fixative for 2 hr at 4 °C, and stored in 0.1 M PB (pH 7.2) buffer at 4 °C. Serial sections of the brainstem were made in the frontal plane at 50 (PhAL) or 100 (BDA) μm using a Vibratome (Leica).

In order to visualize the HRP, free floating sections were first reacted with tetramethylbenzidine (TMB, Sigma) to reveal the location of the retrogradely labeled motoneurons. The TMB reaction product was then stabilized with diaminobenzidine (DAB; Sigma) to produce a brown reaction product (see Perkins et al., 2009 for details). To visualize the BDA labeled axonal arbors, free floating sections were incubated in a solution containing avidin-HRP (Vector Laboratories, Burlingame, CA), followed by incubation with the chromagen, DAB. Addition of cobalt chloride and nickel ammonium sulfate to the DAB solution stained these processes black. To visualize PhaL, free floating sections were first incubated with biotinylated goat anti-PhaL (Cat. No. BA-0224; Vector Laboratories) before being incubated in a solution of avidin-biotin-horseradish peroxidase complex (ABC Vectastain kit; Vector Laboratories Cat# PK-4002, RRID: AB_2336811). Peroxidase activity was then revealed using the aforementioned nickel–cobalt DAB approach, resulting in a black reaction product within labeled axons and axon terminals (see Bohlen et al., 2016 for details). One series containing every third section was reacted for light microscopy and a second reacted series was used to collect samples for electron microscopy. Specifically, retrogradely labeled medial rectus A-, B-, and C-groups were visualized and excised from the second series with the aid of a dissecting microscope (WILD-M8; Leica). These samples were osmicated, *en bloc* stained, sectioned, and stained using standard electron microscopy procedures (see Barnerssoi & May, 2016 for details). The ultrastructure of the labeled areas was photographed using a digital camera on a Joel 1400 electron microscope. The brainstem

sections from both these series were mounted onto gelatinized slides, air-dried, counterstained with cresyl violet, dehydrated, cleared, and coverslipped for microscopic inspection. Labeled axons and cells were plotted and drawn using a Nikon Eclipse 80i (Nikon Instruments, Melville, NY) microscope equipped with a drawing tube, and were photographed using a Nikon Eclipse E600i microscope equipped with a Nikon DS-Ri1 digital camera. In some cases, multiple *z*-axis planes were fused into a single image. The color and contrast of images were digitally adjusted in Photoshop (Adobe) to approximate the viewed image.

3 | RESULTS

Figure 1 shows the distribution of retrogradely labeled medial rectus motoneurons (dots) within the oculomotor nucleus (III) ipsilateral to the injected (left) muscle. There were three populations of medial rectus motoneurons, consistent with many previous reports (Büttner-Ennever & Akert, 1981; Erichsen, Wright, & May, 2014; Porter et al., 1983). The A-group, containing medial rectus SIF motoneurons, was present ventrolaterally within III (Figure 1a–d) and included clusters within the medial longitudinal fasciculus (MLF) (Figure 1c,d). The B-group, containing a second population of medial rectus SIF motoneurons, was observed dorsally within the caudal portion of III (Figure 1d–f). Finally, the C-group, containing medial rectus MIF motoneurons, was found just outside the dorsomedial edge of III and was present for almost all its rostral-caudal extent (Figure 1b–e). In this case, the left cMRF was infused with a large BDA injection that extended from the rostral to caudal pole of the cMRF (Figure 1c–e; insets). There was some spread of tracer rostrally into the piMRF (Figure 1b; inset), dorsally into the nucleus of the posterior commissure (Figure 1e; inset), and medially to the edge of the MLF (Figure 1b,c; insets). Consistent with previous reports (Bohlen et al., 2016; May et al., 2016), there was a bilateral terminal field (stipple) present within the SOA (Figure 1a–f), and terminals were particularly dense around the preganglionic Edinger-Westphal nucleus (EWpg) (Figure 1a–e). The terminals within SOA included a set that completely overlapped the distribution of C-group medial rectus motoneurons (Figure 1a–d). Though much less densely distributed, terminals were also observed bilaterally within the borders of III. Some of these overlapped the distribution of the medial rectus SIF motoneuron populations making up the A-group (Figure 1b–e) and B-group (Figure 1d–f). The pattern described here was consistent across all cases, although the density of labeled terminals varied with the location of the cMRF injection.

The relationship between anterogradely labeled cMRF axon terminals and the retrogradely identified medial rectus MIF motoneurons in the ipsilateral C-group for this case (Figure 1) is further illustrated in Figure 2. Only short lengths of labeled axons were visible in each section in this region, suggesting that they extend in a rostrocaudal direction. The labeled axons were thin, and were rarely observed to branch. The labeled axons were ornamented with small to medium sized boutonal enlargements all along their course. Numerous cMRF axon terminals were observed in close association (arrowheads) with ipsilateral medial rectus C-group motoneurons (Figure 2d). Furthermore, an individual axon often displayed more than one close association with an individual motoneuron or with adjacent motoneurons (Figure 2c). Consequently, nearly every C-group medial rectus motoneuron

had labeled cMRF terminals in close association with it (Figure 2c,d), and most displayed multiple close associations with several cMRF axons.

Figure 3 illustrates cMRF projections to the ipsilateral A-group (Figure 3c–e) and B-group (Figure 3f,g) medial rectus SIF motoneurons from the same BDA case illustrated in Figure 1. The general morphology of the labeled axons was similar to that seen in the SOA, although there were far fewer axons present. Individual axons rarely made more than one or two contacts on an individual motoneuron, although this was more common for B-group cells (Figure 3f). Nevertheless, close associations (arrowheads) could be observed between these cMRF axon terminals and both A-group motoneurons (Figure 3c–e) and B-group motoneurons (Figure 3f,g). In comparison to the density of close associations present on C-group motoneurons, close associations were much less common for A-group motoneurons and somewhat less common for B-group motoneurons, so some motoneurons did not receive inputs (Figure 3c,f).

Figure 4 shows photomicrographs of motoneuron and axon labeling seen in the three ipsilateral subgroups. The retrogradely labeled medial rectus motoneurons display reaction product throughout their cell bodies and extending out into their dendrites. The motoneurons in the C-group (Figure 4a,b) have smaller somata than those in the A-group (Figure 4c,d) or B-group (Figure 4e,f). Note the much greater density of axons around the C-group motoneurons. The labeled axons are quite thin, and are studded with small to medium sized *en passant* boutons. In these examples, C-group motoneurons displayed numerous closely associated terminal boutons (arrowheads, Figure 4a,b). These close associations could be observed on both the somata and dendrites. Close associations were also observed on the ipsilateral A-group (Figure 4c,d) and B-group (Figure 4e,f) medial rectus motoneurons. However, far fewer close associations were present for these SIF populations.

In order to verify that the BDA labeled terminals we observed did originate from the cMRF, PhaL was injected into the cMRF because this tracer has little to no fiber-of-passage uptake (Gerfen & Sawchenko, 1984; Wouterlood & Groenewegen, 1985). In the case shown in Figure 5, PhaL was injected into the left cMRF, and then the left medial rectus muscle was injected to retrogradely label medial rectus motoneurons (dots) on the same side. The PhaL injection site was small, and centrally placed within the cMRF (Figure 5d; inset), with some spread along the needle tract dorsally into the nucleus of the posterior commissure (nPC) and thalamus. Although the PhaL injection resulted in fewer labeled axons compared to the BDA case, the bilateral pattern of terminal distribution (stipple) was very similar, and provided the same result. The ipsilateral terminal field was observed to overlap the distribution of C-group motoneurons (Figure 5b–e). Labeled axons were also observed within III, overlapping with the distribution of the ipsilateral A- (Figure 5a–c) and B-group (Figure 5d–f) motoneurons, although these were far less concentrated than over the C-group. Only a very few labeled terminals were observed in contralateral III at the location of the A- and B-groups.

Figure 6 shows anterogradely labeled axon terminals in close association with retrogradely labeled medial rectus MIF motoneurons in the ipsilateral C-group from the same PhaL case as illustrated in Figure 5. Inspection of this area revealed numerous axon terminals in close

association with these motoneurons (Figure 6c–f). They often had more than one boutonal enlargement in close association (arrowhead) with an individual or several ipsilateral C-group medial rectus motoneurons (Figure 6c–f). In addition, nearly every C-group medial rectus motoneuron received multiple labeled close associations. Thus, the result was essentially the same as with the BDA injection (Figure 2).

Figure 7 illustrates cMRF projections to the ipsilateral A-group (Figure 7b–d) and B-group (Figure 7e–g) medial rectus SIF motoneurons from the same PhaL case (Figure 5). In contrast to the C-group, the axons were scattered and far fewer in number within the A-group (Figure 7c) and somewhat fewer in number in the B-group (Figure 7f). Axonal boutons were observed in close association with A-group motoneurons (arrowheads, Figure 7c,d), but not all cells received a close association (Figure 7c). More labeled axons were present among the B-group motoneurons (Figure 7f) and most cells received several close associations (arrowheads, Figure 7f,g). Again, the results were very similar to BDA findings of a more sparse input (Figure 3).

The photomicrographs in Figure 8 show examples of close associations between PhaL labeled axon terminals and retrogradely labeled A-, B-, and C-group medial rectus motoneurons from this case (Figure 5). Inspection of the neuropil surrounding the labeled cells reveals differences in the density of cMRF axon terminals projecting to the three medial rectus populations. The C-group region (Figure 8a) clearly receives the majority of axon terminals, while the region around the A-group (Figure 8c) receives the least. In general, the PhaL labeled axons had thin diameters with regularly spaced, *en passant* boutons. Numerous close associations (arrowheads) were observed on the soma and dendrites of C-group (Figure 8a) motoneurons, while relatively fewer were observed in close association with A- or B-group motoneurons (Figure 8c,b, respectively).

Previously, we noted that the terminal field within the SOA was bilateral within the region populated by C-group motoneurons (Bohlen et al., 2015). In order to determine if the cMRF has a projection to motoneurons on the contralateral side, BDA was injected into the left cMRF and WGA-HRP or ChTB-HRP was injected into the right medial rectus muscle to retrogradely label motoneurons on the side contralateral to the cMRF injection site. The BDA injection site and resultant terminal distribution (stipple) are shown in combination with the location of the retrogradely labeled medial rectus motoneurons (dots) in Figure 9. The injection site was well confined to the lateral half of the left cMRF (Figure 9c–e). This lateral injection site resulted in a less dense terminal field within the SOA, a finding consistent with our previous report (Bohlen et al., 2015). Despite the decrease in terminal density, there was still significant overlap between this contralateral projection and the distribution of C-group medial rectus motoneurons on the right (Figure 9b–e). In contrast to the ipsilateral terminal fields in III on the left, there appeared to be only a few labeled axons in the region containing the A-group (Figure 9a–d) or B-group motoneurons on the right side (Figure 9e,f).

Figure 10 illustrates close associations between BDA labeled axon terminals from the left cMRF and medial rectus MIF motoneurons within the right C-group from the case illustrated in Figure 9. Like the cMRF projections to the ipsilateral side (Figure 4), cMRF

axons projecting to the contralateral side were very dense around these C-group motoneurons. Many axons made at least one close association with a labeled C-group motoneuron and often axons were observed making multiple close associations with multiple C-group motoneurons (Figure 10c,d). Every labeled contralateral C-group medial rectus motoneuron received close associations from cMRF boutons, and in most cases, they received numerous close associations from multiple axons.

Figure 11 illustrates cMRF projections to the contralateral A-group (Figure 11e,f) and B-group (Figure 11c,d) medial rectus SIF motoneurons from the same case. The density of cMRF projections within the contralateral A- and B-group motoneurons was far less than observed for the ipsilateral A- and B-groups. Very few labeled axons were present within the A-group. In fact, only one short axon was observed with boutonal enlargements in the illustrated sample section (Figure 11e,f). There were more labeled axons within the contralateral B-group region, but these axons were quite dispersed. Just a few B-group motoneurons received one or two close associations from axons labeled from the contralateral cMRF (Figure 11c,d).

Photomicrographs of cMRF axon terminal arbors and medial rectus motoneurons located contralateral to the cMRF injection site are shown in Figure 12. Numerous close associations could be observed on the soma and dendrites of a contralateral C-group medial rectus motoneuron (Figure 12a; arrowhead). An example of a contralateral B-group medial rectus motoneuron is shown with somal close associations (Figure 12b; arrowhead). This example was one of the most heavily contacted cells observed. Finally, an example of an A-group motoneuron with an axon traversing one of its dendrites with no boutons or evidence of a close association is shown in Figure 12c (arrowhead). Note the differences in the density of terminals in the surrounding neuropil between C-group (Figure 12a), B-group (Figure 12b), and A-group (Figure 12c).

In order to confirm that the close associations observed at the light microscopic level included true synaptic contacts, samples from each subgroup were taken for electron microscopy. Electron micrograph examples of anterogradely labeled cMRF terminals synaptically contacting retrogradely labeled medial rectus motoneurons are shown in Figure 13. Retrogradely labeled somatic and dendritic (Den*) profiles from motoneurons were identified by the presence of flocculent electron dense reaction product in their cytoplasm (Figure 13a–f, arrows). The anterogradely labeled axon terminals (At*) (Figure 13b–f) were identified as having a cytoplasm that was more electron dense compared to other nonlabeled terminals (At) (Figure 13a, c) in the vicinity. This anterograde label was often evenly distributed throughout the terminal cytoplasm, and in more lightly labeled examples, it appeared to aggregate most densely at the cytoplasmic edges of internal structures like vesicles and mitochondria (Figure 13f). Anterogradely labeled cMRF axon terminals were observed making synaptic contacts (arrowheads) onto medial rectus MIF motoneurons in C-group both ipsilateral to cMRF injection site (Figure 13a,b) and contralateral to the cMRF injection (Figure 13c). In addition, cMRF synaptic terminals were observed to contact retrogradely labeled ipsilateral medial rectus SIF motoneurons within B-group (Figure 13d) and A-group (Figure 13e,f).

4 | DISCUSSION

This study provides evidence, summarized in Figure 14, that the cMRF has a strong, direct, and bilateral projection to medial rectus MIF motoneurons in the C-group. The results also indicate that the cMRF has a weaker, ipsilateral projection to medial rectus SIF motoneurons within the A- and B-groups. The ultrastructural evidence proves that a mono-synaptic linkage exists for all three subgroups. The density of the projection of cMRF terminals on the C-group somata and dendrites suggests that this projection is able to drive the activity of these motoneurons, but the pattern of inputs to the A- and B- group cells indicates a more modulatory role (Figure 14). Two critical conclusions drawn from these findings are discussed below. First, the pattern of cMRF inputs to the MIF and SIF medial rectus motoneurons differ, indicating a difference in their functional roles during eye movements. Second, the dominant bilateral cMRF projection to both C-group and EWpg suggests that medial rectus MIF motoneurons may play a role in vergence movements during near triad actions.

4.1 | Technical considerations

One consideration in using tracers is spread outside the targeted area. In this study, the adjacent regions of particular concern include the piMRF, rostrally, the nucleus of the posterior commissure, dorsally, the decussation of the superior cerebellar peduncle, ventrally, and the fibers of the MLF, medially. The piMRF and the nucleus of the posterior commissure are believed to be associated with vertical gaze control (Chen & May, 2007; Perkins et al., 2014; Waitzman et al., 2000a, 2000b). Perhaps for this reason, those cases with spread of tracer into these regions showed little difference in the pattern of close associations with medial rectus motoneurons. With regard to tracer spillover into the MLF and the brachium conjunctivum, or uptake by predorsal bundle axons traversing the cMRF, we utilized PhaL as a tracer in one case, rather than BDA, because PhAL is reputed to not be picked up by fibers (Gerfen & Sawchenko, 1984; Wouterlood & Groenewegen, 1985). This case had essentially the same pattern of terminals around the ipsilateral medial rectus subgroups and the area of the contralateral C-group motoneurons as did the BDA cases (Figures 1 and 5), although labeled predorsal bundle axons were not present in the pons. It did differ in that few, if any, terminals were present in contralateral III. This suggests the limited terminal labeling seen adjacent to contralateral A-and B-group cells following BDA injections may come from some source other than the cMRF. An additional point worth noting is that negative findings about synaptic contacts on the motoneurons need to be considered in light of the fact that much of their dendritic field was not visualized. Conversely, given that there are relatively few synaptic contacts on the somata and proximal dendrites of C-group motoneurons (Erichsen et al., 2014), the considerable fraction of contacts observed indicates that cMRF terminals may provide the main axosomatic input to these cells.

4.2 | Implications for MIF function

At the outset of this investigation, a primary goal was to determine whether MIF motoneurons received different inputs than SIF motoneurons. We have partially confirmed this point in that there is a large, bilateral projection to the medial rectus MIF motoneurons

within the C-group and a minor, ipsilateral projection to SIF medial rectus motoneurons (Figure 14). The extent of this difference suggests that the cMRF projection to MIF motoneurons plays a different role than the cMRF projection to the SIF motoneurons, and that the two target populations are likely to have different physiological functions. Other projections may selectively terminate on MIF or SIF motoneuronal populations in primates. Wasicky et al. (2004) found that the superior vestibular nucleus has projections that only overlie the A- and B-groups. In the same study, anterograde tracer injections into the pretectal area labeled terminals in areas containing MIF motoneurons. Anterograde tracers injected into the interposed and fastigial nuclei of the cerebellum also result in terminal fields in the SOA that overlie the C-group, but not the A- and B-group (May, Porter, & Gamlin, 1992). Conversely, not all inputs show segregation between the MIF and SIF motoneurons. For example, the abducens internuclear axons terminate over all three medial rectus populations (Büttner-Ennever & Akert, 1981; Wasicky et al., 2004). It is interesting that both the abducens internuclear neurons and the cMRF are believed to play roles in horizontal saccadic eye movements, and that we have shown here that the cMRF also projects to all three groups. Retrograde trans-synaptic tracer techniques have also been used to examine this question. Ugolini et al. (2006) injected rabies virus into either the macaque lateral rectus muscle insertion or belly to reveal that lateral rectus MIF motoneurons lack several inputs that the SIF motoneurons receive, including projections from the paramedian pontine reticular formation. Lateral rectus MIF motoneurons did receive monosynaptic inputs from the cMRF, SOA, nucleus prepositus hypoglossi, and portions of the medial vestibular nucleus. The present results confirmed the evidence for premotor cells in cMRF that project to the MIF motoneurons, but also demonstrated a cMRF input to SIF motoneurons. Interestingly, the cMRF projection to both medial and lateral rectus MIF motoneurons is bilateral.

These differences in input suggest that the MIF and SIF motoneurons may have distinct patterns of activity and function. Unfortunately, no one has, to date, recorded from an identified MIF motoneuron. In fact, there is no evidence for a separate subpopulation of extraocular motoneurons that preferentially displays tonic activity, as one might expect for cells supplying MIFs, since these fibers seem specialized for graded and tonic contraction. Instead, most neurophysiological investigations have reported that all recorded extraocular motoneurons for a given extraocular muscle are involved in all actions of that muscle (Fuchs & Luschei, 1970; Henn & Cohen, 1973; Keller & Robinson, 1972; Miller, Davison, & Gamlin, 2011; Schiller, 1970; Van Horn & Cullen, 2009). It is possible that the small, peripherally located, MIF motoneurons may have been missed; particularly, if their firing is so dissimilar from SIF motoneuron activity that they were dismissed as nonmotoneurons. Alternatively, the MIF motoneuron pattern of activity may be similar to that of SIF motoneurons, and any difference in action is produced solely by muscle fiber characteristics. In fact, Nelson et al. (1986) showed that MIFs produce a slow graded response to high frequency stimulation. Certainly, the present data indicate that MIF motoneurons are probably supplied with a saccade-related burst of activity from the cMRF.

MIF contraction is reported to take place at a much lower stimulus frequency (~30/s) compared to the rate required to induce SIF contraction (350–600/s) (Bach-y-Rita & Ito, 1966; Buller & Lewis, 1965; Hess & Pilar, 1963). Based on this, Fuchs and Luschei (1971)

concluded that the MIFs do not serve any role in eye movement because stimulation of the abducens nerve at a rate of 30/s produced no detectable effect on muscle tension. However, these experiments used monkeys anesthetized with barbiturates, and slow (oxidative) muscle fibers, like MIFs, are significantly more impaired by sodium pentobarbital (Taylor, Abresch, Lieberman, Fowler, & Portwood, 1984). Thus, direct barbiturate effects on the MIF muscle fibers may have masked the stimulation effects. Furthermore, it seems counterintuitive that a subgroup that makes up 10–20% of the extraocular muscle fibers would have no role in eye movements, and not produce any muscle tension. In fact, microstimulation of the area dorsal to III results in bilateral pupillary constriction, with depression and adduction of the eye (Jampel, 1967; Jampel & Mindel, 1967). This most likely reflects the bilateral activation of EWpg and the C-group.

The current notion is that MIFs and MIF motoneurons serve slow movements, like smooth pursuit, or tonic behaviors, like fixation (see Spencer & Porter, 2006 for review). In this light, an input from the cMRF might seem surprising, as there is considerable evidence for saccade-related activity and little evidence for vestibular slow phase or pursuit-related activity in this region (Cohen et al., 1986; Pathmanathan, Cromer, Cullen, & Waitzman, 2006a; Pathmanathan, Presnell, Cromer, Cullen, & Waitzman, 2006b; Waitzman et al., 1996). However, many cMRF cells maintain high rates of activity after a saccade is completed (Waitzman et al., 1996). Such cells might be appropriate to provide input to MIF motoneurons, if they help maintain eye position. A more recent study by Waitzman, Van Horn and colleagues (2008) indicates that when disjunctive saccades are made, cMRF cells adapt the duration of their firing to match the slower eye speeds. This type of input might be appropriate to drive MIF motoneurons.

The initial cMRF stimulation studies also showed that bilateral activation produced fixation (Cohen et al., 1985, 1986) and the majority of cMRF neurons display high rates of tonic activity (Waitzman et al., 1996). In fact, a cMRF projection to the omnipause cells in the nucleus raphe interpositus, whose activity correlates with fixation, has been reported (Wang et al., 2013), but this projection is predominantly GABAergic, which would tend to suggest it suppresses fixation. Perhaps the cMRF's premotor input actually turns off the tonic fixation-related activity of MIF motoneurons during horizontal saccades. If this were the case, one might expect an equivalent projection to abducens MIF motoneurons. Such a projection is present (Ugolini et al., 2006), but seems relatively sparse (Bohlen et al., 2016).

Based on the distribution of the medial rectus C-group dendrites within the SOA and EWpg, it has been suggested that medial rectus MIF motoneurons are involved in vergence movements (Erichsen et al., 2014; Tang, Büttner-Ennever, Mustari, & Horn, 2015; Figure 14). Our work on cMRF projections supports this contention, as we have observed bilateral inputs with similar densities and morphologies terminating on preganglionic motoneurons in EWpg and on medial rectus MIF motoneurons (May et al., 2016, present results). Furthermore, medial rectus MIF motoneuron dendrites receive considerable input within EWpg (Erichsen et al., 2014), so the axosomatic contacts from cMRF terminals described here may simply be an extension of the cMRF projection they receive within this adjacent nucleus. Certainly, it is noteworthy that MIF contraction speeds and lens accommodation rates are well matched. Indeed, the actions of all the components of the near triad are quite

slow (Judge & Cumming, 1986; Mays, Porter, Gamlin, & Tello, 1986), and while disconjugate saccades are faster than symmetric vergence movements, they are still slower than conjugate ones (Enright, 1984; Maxwell & King, 1992). Perhaps this match occurs, in part, because a larger role is played by MIF fibers in accomplishing the movement and maintaining the position of the eyes during vergence. It also should be noted that during fixation, the eyes are not actually perfectly stable. Slow drifts, physiological tremor, and microsaccades occur during fixation and play an important role in keeping retinal photoreceptors from fading (Martinez-Conde, Macknik, Troncoso, & Dyar, 2006; Otero-Millan, Macknik, & Martinez-Conde, 2014). Consideration must be given to the possibility that MIFs might play a role in these movements, particularly drift.

A portion of the MIFs in frontally eyed species have specialized end organs called palisade endings located at the myotendinous junction (Ruskell, 1978). Palisade endings were assumed to be sensory structures, compensating for a general lack of conventional proprioceptive receptors (muscle spindles) in the extraocular musculature (Billig, Buisseret-Delmas, & Buisseret, 1997; Donaldson, 2000; Ruskell, Kjellevold Haugen, Bruenech, & van der Werf, 2005; Steinbach, 1987; Weir, Knox, & Dutton, 2000). However, palisade endings also show features that correlate with a motor function: for example, they contain vesicles and are immunoreactive for cholinergic markers (Blumer et al., 2009; Eberhorn et al., 2005; Konakci et al., 2005a, 2005b; Lukas et al., 2000). Furthermore, injections of anterograde tracer into the extraocular motor nuclei label palisade endings, indicating the source of these features lies in the MIF motoneuron pools (Lienbacher, Mustari, Ying, Büttner-Ennever, & Horn, 2011; Zimmermann, May, Pastor, Streicher, & Blumer, 2011; Zimmermann et al., 2013). Since nearly all C-group motoneurons were heavily invested with cMRF terminals, it stands to reason that those supplying palisade endings received input. It has recently been shown that the medial rectus muscles of frontally eyed animals display a particularly enriched population of palisade endings, leading to the idea that this enrichment plays a critical role in maintaining convergence during stereopsis (Blumer et al., 2016). Our findings that the cMRF provides heavy input to motoneurons in both the EWpg and C-group is in agreement with this proposal.

4.3 | Vergence-accommodation cross-coupling

Any change along the *Z*-axis view necessitates a change in lens accommodation in order for the foveated target to be in focus (Hung, 2001). Retinal disparity signals can drive both vergence and lens accommodation, a pairing known as convergence-accommodation (Fincham & Walton, 1957). Conversely, an out-of-focus retinal image (i.e., accommodative error) also drives both accommodation and vergence, a pairing known as accommodation-convergence (Morgan, 1968). Based on behavioral data from human psychophysics studies, Hung (1997) proposed a dual-feedback model to explain these interactions. A link between the two systems has been substantiated through neurophysiological recordings, which revealed premotor neurons, termed midbrain near response cells, whose activity is related to both convergence and accommodation (Judge & Cumming, 1986; Mays, 1984; Zhang, Mays, & Gamlin, 1992). Our examination of cMRF projections (Bohlen et al., 2016, present results) indicates that like midbrain near response cells, the cMRF also has projections to both medial rectus motoneurons and preganglionic motoneurons in EWpg. The presence of

this second, paired premotor projection may help explain why lens accommodation and vergence are so intimately linked. In fact, although we have illustrated the cMRF projections to EWpg and the C-group with separate arrows in Figure 14, we feel it is likely that they originate from the same cells.

Conversely, A- and B-group SIF motoneurons are positioned with their dendrites located primarily within III (Erichsen et al., 2014; Tang et al., 2015). Thus, they may be able to drive conjugate gaze along the *X*-axis due to inputs that do not change lens accommodation. While these cells were shown to receive cMRF input in the present study, this input differed in its density and was ipsilateral, not bilateral, suggesting it serves a conjugate gaze role. Further experiments are needed to determine whether the cMRF projection to each of its motoneuron targets comes from separate sets of neurons.

4.4 | Role of the cMRF

The heavy, bilateral projection by the cMRF to EWpg and to medial rectus MIF motoneurons in C-group suggest that the cMRF plays a role in the near triad (Bohlen et al., 2016; present results). This seems to run counter to the original reports by Cohen et al. (1984, 1985) that cMRF stimulation produces conjugate contraversive saccades. Furthermore, other studies have suggested that the midbrain near response cells responsible for vergence changes are located in the SOA (Das, 2011, 2012; Mays, 1984). However, the description of vergence velocity cells seems to place them in the medial cMRF (Mays et al., 1986). So another point in need of investigation is the extent to which the premotor neurons in the cMRF and the near response neurons in SOA represent distinct populations.

More recently, Waitzman et al. (2008) found that when the cMRF was electrically activated, it could elicit either conjugate or disjunctive eye movements, depending on the microstimulation point. Perhaps the conjugate areas provide the SIF motoneuron projection and the disjunctive areas provide the MIF motoneuron projection. In this same study, cMRF neuron activity was correlated with the movement of an individual eye during disjunctive saccades. If these were premotor neurons, then is possible that the projections to the ipsilateral and contra-lateral C-group originate from separate pools of premotor neurons within the cMRF (Figure 14). For a conjugate saccade, the ipsilateral medial rectus motoneuron projection would presumably be excitatory and the contralateral projection, inhibitory. However, if the cMRF projection is indeed modulating gaze with respect to target distance during disjunctive saccades, as suggested by Waitzman et al. (2008), a more complex pattern of inhibition or excitation may be needed. Since the new target may be closer or further away from the current fixation point, it might require either a convergent or divergent modification of the conjugate plan of action for each eye.

Acknowledgments

Funding information

NIH grant, Grant/Award Number: # EY014263 (to P.J.M. and S.W.)

We would like to thank Ms. Jinrong Wei for her assistance in the surgeries and for the histological preparation of the material. We also acknowledge the assistance of Jeremy Sullivan for processing material for electron microscopy and assisting with its observation. Finally, we thank Drs. Paul Gamlin and Julie Quinet for helpful

comments on earlier drafts of the manuscript. This study was done in partial fulfillment of Dr. Bohlen's thesis requirements.

Abbreviations

At	axon terminal
At*	labeled axon terminal
BC	brachium conjunctivum
BDA	biotinylated dextran amine
CC	caudal central subdivision of III
ChTB-HRP	choleratoxin B subunit conjugated to HRP
cMRF	central MRF
DAB	diaminobenzidine
Den	dendrite
Den*	labeled dendrite
EWcp	centrally projecting Edinger-Westphal nucleus
EWpg	preganglionic Edinger-Westphal nucleus
HRP	horseradish peroxidase
III	oculomotor nucleus
InC	interstitial nucleus of Cajal
MIF	multiply innervated fiber
MLF	medial longitudinal fasciculus
MRF	mesencephalic reticular formation
nPC	nucleus of the posterior commissure
PAG	periaqueductal gray
PhaL	*Phaseolus vulgaris* leucoagglutinin
piMRF	peri-InC portion of the MRF
SIF	singly innervated fiber
SOA	supraoculomotor area
TMB	tetramethylbenzidine
WGA-HRP	wheat germ agglutinin conjugated to HRP

References

Appell PP, Behan M. Sources of subcortical GABAergic projections to the superior colliculus in the cat. Journal of Comparative Neurology. 1990; 302:143–158. [PubMed: 2086611]

Bach-y-Rita P, Ito F. In vivo studies on fast and slow muscle fibers in cat extraocular muscles. Journal of General Physiology. 1966; 49:1177–1198. [PubMed: 5924106]

Bach-y-Rita P, Lennerstrand G, Alvarado J, Nichols K, McHolm G. Extraocular muscle fibers: Ultrastructural identification of ion-tophoretically labeled fibers contracting in response to succinylcholine. Investigative Ophthalmology & Visual Science. 1977; 16:561–565. [PubMed: 863618]

Barnerssoi, M., May, PJ. Postembedding immunohistochemistry for inhibitory neurotransmitters in conjunction with neuroanatomical tracers. In: Van Bockstaele, RJ., editor. Transmission electron microscopy methods for understanding the brain. Vol. 115. New York: Springer Science; 2016. p. 181-203.

Bender, MB., Shanzer, S. Oculomotor pathways defined by electrical stimulation and lesions in the brainstem of monkey. In: Bender, MB., editor. The oculomotor System. 1. New York, NY: Hoeber Medical Division, Harper & Row, USA; 1964. p. 81-140.

Billig I, Buisseret-Delmas C, Buisseret P. Identification of nerve endings in cat extraocular muscles. The Anatomical Record. 1997; 248:566–575. [PubMed: 9268145]

Blumer R, Konakci KZ, Pomikal C, Wieczorek G, Lukas JR, Streicher J. Palisade endings: Cholinergic sensory organs or effector organs? Investigative Ophthalmology & Visual Science. 2009; 50:1176–1186. [PubMed: 18936148]

Blumer R, Maurer-Gesek B, Gesslbauer B, Blumer M, Pechriggl E, Davis-Lopez de Carrizosa MA, … Pastor AM. Palisade endings are a constant feature in the extraocular muscles of frontal-eyed, but not lateral-eyed, animals. Investigative Ophthalmology & Visual Science. 2016; 57:320–331. [PubMed: 26830369]

Bohlen MO, Warren S, May PJ. Central mesencephalic reticular formation projections to horizontal gaze motoneurons: A green light or red? Society Neuroscience Abstracts. 2015 417.05/N39.

Bohlen MO, Warren S, May PJ. A central mesencephalic reticular formation projection to the supraoculomotor area in macaque monkeys. Brain Structure and Function. 2016; 221:2209–2229. [PubMed: 25859632]

Bondi AY, Chiarandini DJ. Morphologic and electrophysiologic identification of multiply innervated fibers in rat extraocular muscles. Investigative Ophthalmology & Visual Science. 1983; 24:516–519. [PubMed: 6187707]

Buller AJ, Lewis DM. The rate of tension development in isometric tetanic contractions of mammalian fast and slow skeletal muscle. Journal of Physiology. 1965; 176:337–354. [PubMed: 14288512]

Büttner-Ennever JA, Akert K. Medial rectus subgroups of the oculomotor nucleus and their abducens internuclear input in the monkey. Journal of Comparative Neurology. 1981; 197:17–27. [PubMed: 6894456]

Büttner-Ennever JA, Horn AK, Scherberger H, D'Ascanio P. Motoneurons of twitch and nontwitch extraocular muscle fibers in the abducens, trochlear, and oculomotor nuclei of monkeys. Journal of Comparative Neurology. 2001; 438:318–335. [PubMed: 11550175]

Chen B, May PJ. The feedback circuit connecting the superior colliculus and central mesencephalic reticular formation: A direct morphological demonstration. Experimental Brain Research. 2000; 131:10–21. [PubMed: 10759167]

Chen B, May PJ. Premotor circuits controlling eyelid movements in conjunction with vertical saccades in the cat: II. interstitial nucleus of Cajal. Journal of Comparative Neurology. 2007; 500:676–692. [PubMed: 17154251]

Chiarandini DJ, Davidowitz J. Structure and function of extraocular muscle fibers. Current Topics in Eye Research. 1979; 1:91–142. [PubMed: 400680]

Chiarandini DJ, Stefani E. Electrophysiological identification of two types of fibres in rat extraocular muscles. Journal of Physiology. 1979; 290:453–465. [PubMed: 469787]

Cohen B, Büttner-Ennever JA. Projections from the superior colliculus to a region of the central mesencephalic reticular formation (cMRF) associated with horizontal saccadic eye movements. Experimental Brain Research. 1984; 57:167–176. [PubMed: 6519224]

Cohen B, Matsuo V, Fradin J, Raphan T. Horizontal saccades induced by stimulation of the central mesencephalic reticular formation. Experimental Brain Research. 1985; 57:605–616. [PubMed: 3979501]

Cohen B, Waitzman DM, Büttner-Ennever JA, Matsuo V. Horizontal saccades and the central mesencephalic reticular formation. Progress in Brain Research. 1986; 64:243–256. [PubMed: 3726146]

Cowie RJ, Smith MK, Robinson DL. Subcortical contributions to head movements in macaques. II. Connections of a medial pontomedullary head-movement region. Journal of Neurophysiology. 1994; 72:2665–2682. [PubMed: 7534824]

Cromer JA, Waitzman DM. Neurones associated with saccade metrics in the monkey central mesencephalic reticular formation. Journal of Physiology. 2006; 570:507–523. [PubMed: 16308353]

Cromer JA, Waitzman DM. Comparison of saccade-associated neuronal activity in the primate central mesencephalic and paramedian pontine reticular formations. Journal of Neurophysiology. 2007; 98:835–850. [PubMed: 17537904]

Das VE. Cells in the supraoculomotor area in monkeys with strabismus show activity related to the strabismus angle. Annals of the New York Academy of Sciences. 2011; 1233:85–90. [PubMed: 21950980]

Das VE. Responses of cells in the midbrain near-response area in monkeys with strabismus. Investigative Ophthalmology & Visual Science. 2012; 53:3858–3864. [PubMed: 22562519]

Donaldson IM. The functions of the proprioceptors of the eye muscles. Philosophical Transactions of the Royal Society of London B: Biological Sciences. 2000; 355:1685–1754. [PubMed: 11205338]

Eberhorn AC, Büttner-Ennever JA, Horn AK. Identification of motoneurons supplying multiply- or singly-innervated extraocular muscle fibers in the rat. Neuroscience. 2006; 137:891–903. [PubMed: 16330150]

Eberhorn AC, Horn AK, Eberhorn N, Fischer P, Boergen KP, Büttner-Ennever JA. Palisade endings in extraocular eye muscles revealed by SNAP-25 immunoreactivity. Journal of Anatomy. 2005; 206:307–315. [PubMed: 15733303]

Edwards SB. Autoradiographic studies of the projections of the midbrain reticular formation: Descending projections of nucleus cuneiformis. Journal of Comparative Neurology. 1975; 161:341–358. [PubMed: 50329]

Edwards SB, de Olmos JS. Autoradiographic studies of the projections of the midbrain reticular formation: Ascending projections of nucleus cuneiformis. Journal of Comparative Neurology. 1976; 165:417–431. [PubMed: 1262539]

Enright JT. Changes in vergence mediated by saccades. Journal of Physiology. 1984; 350:9–31. [PubMed: 6747862]

Erichsen JT, Wright NF, May PJ. Morphology and ultra-structure of medial rectus subgroup motoneurons in the macaque monkey. Journal of Comparative Neurology. 2014; 522:626–641. [PubMed: 23897455]

Fincham EF, Walton J. The reciprocal actions of accommodation and convergence. Journal of Physiology. 1957; 137:488–508. [PubMed: 13463783]

Fuchs AF, Luschei ES. Firing patterns of abducens neurons of alert monkeys in relationship to horizontal eye movement. Journal of Neurophysiology. 1970; 33:382–392. [PubMed: 4985724]

Fuchs AF, Luschei ES. Development of isometric tension in simian extraocular muscle. Journal of Physiology. 1971; 219:155–166. [PubMed: 5003481]

Gerfen CR, Sawchenko PE. An anterograde neuroanatomical tracing method that shows the detailed morphology of neurons, their axons and terminals: Immunohistochemical localization of an axonally transported plant lectin, Phaseolus vulgaris leucoagglutinin (PHA-L). Brain Research. 1984; 290:219–238. [PubMed: 6198041]

Graf W, Gerrits N, Yatim-Dhiba N, Ugolini G. Mapping the oculomotor system: The power of transneuronal labelling with rabies virus. European Journal of Neuroscience. 2002; 15:1557–1562. [PubMed: 12028367]

Grantyn A, Grantyn R. Axonal patterns and sites of termination of cat superior colliculus neurons projecting in the tecto-bulbo-spinal tract. Experimental Brain Research. 1982; 46:243–256. [PubMed: 7095033]

Handel A, Glimcher PW. Response properties of saccade-related burst neurons in the central mesencephalic reticular formation. Journal of Neurophysiology. 1997; 78:2164–2175. [PubMed: 9325383]

Harting JK. Descending pathways from the superior colliculus: An autoradiographic analysis in the rhesus monkey (*Macaca mulatta*). Journal of Comparative Neurology. 1977; 173:583–612. [PubMed: 404340]

Henn V, Cohen B. Quantitative analysis of activity in eye muscle motoneurons during saccadic eye movements and positions of fixation. Journal of Neurophysiology. 1973; 36:115–126. [PubMed: 4196201]

Hess A, Pilar G. Slow fibres in the extraocular muscles of the cat. Journal of Physiology. 1963; 169:780–798. [PubMed: 14103560]

Hung GK. Quantitative analysis of the accommodative convergence to accommodation ratio: Linear and nonlinear static models. IEEE Transactions on Biomedical Engineering. 1997; 44:306–316. [PubMed: 9125813]

Hung, GK. Models of oculomotor control. River Edge, NJ: World Scientific Publishing Co. Pte. Ltd; 2001.

Jacoby J, Chiarandini DJ, Stefani E. Electrical properties and innervation of fibers in the orbital layer of rat extraocular muscles. Journal of Neurophysiology. 1989; 61:116–125. [PubMed: 2783961]

Jampel RS. Multiple motor systems in the extraocular muscles of man. Investigative Ophthalmology. 1967; 6:288–293. [PubMed: 4961066]

Jampel RS, Mindel J. The nucleus for accommodation in the midbrain of the macaque. Investigative Ophthalmology. 1967; 6:40–50. [PubMed: 4959576]

Judge SJ, Cumming BG. Neurons in the monkey midbrain with activity related to vergence eye movement and accommodation. Journal of Neurophysiology. 1986; 55:915–930. [PubMed: 3711972]

Keller EL, Robinson DA. Abducens unit behavior in the monkey during vergence movements. Vision Research. 1972; 12:369–382. [PubMed: 4623266]

Konakci KZ, Streicher J, Hoetzenecker W, Blumer MJ, Lukas JR, Blumer R. Molecular characteristics suggest an effector function of palisade endings in extraocular muscles. Investigative Ophthalmology & Visual Science. 2005a; 46:155–165. [PubMed: 15623769]

Konakci KZ, Streicher J, Hoetzenecker W, Haberl I, Blumer MJ, Wieczorek G, … Blumer R. Palisade endings in extraocular muscles of the monkey are immunoreactive for choline acetyltransferase and vesicular acetylcholine transporter. Investigative Ophthalmology & Visual Science. 2005b; 46:4548–4554. [PubMed: 16303947]

Langer TP, Kaneko CR. Brainstem afferents to the omni-pause region in the cat: A horseradish peroxidase study. Journal of Comparative Neurology. 1984; 230:444–458. [PubMed: 6520245]

Langer TP, Kaneko CR. Brainstem afferents to the oculomotor omnipause neurons in monkey. Journal of Comparative Neurology. 1990; 295:413–427. [PubMed: 2351760]

Lienbacher K, Mustari M, Ying HS, Büttner-Ennever JA, Horn AK. Do palisade endings in extraocular muscles arise from neurons in the motor nuclei? Investigative Ophthalmology & Visual Science. 2011; 52:2510–2519. [PubMed: 21228383]

Lukas JR, Blumer R, Denk M, Baumgartner I, Neuhuber W, Mayr R. Innervated myotendinous cylinders in human extraocular muscles. Investigative Ophthalmology & Visual Science. 2000; 41:2422–2431. [PubMed: 10937549]

Lynch GS, Frueh BR, Williams DA. Contractile properties of single skinned fibres from the extraocular muscles, the levator and superior rectus, of the rabbit. Journal of Physiology. 1994; 475:337–346. [PubMed: 8021839]

Martinez-Conde S, Macknik SL, Troncoso XG, Dyar TA. Microsaccades counteract visual fading during fixation. Neuron. 2006; 49:297–305. [PubMed: 16423702]

Maxwell JS, King WM. Dynamics and efficacy of saccade-facilitated vergence eye movements in monkeys. Journal of Neurophysiology. 1992; 68:1248–1260. [PubMed: 1432082]

May PJ, Horn AK, Mustari M, Warren S. Central mesencephalic reticular formation projections onto oculomotor motoneurons. Society Neuroscience Abstracts. 2011 699.01/PP22.

May PJ, Porter JD, Gamlin PD. Interconnections between the primate cerebellum and midbrain near-response regions. Journal of Comparative Neurology. 1992; 315:98–116. [PubMed: 1371782]

May PJ, Warren S, Bohlen MO, Barnerssoi M, Horn AK. A central mesencephalic reticular formation projection to the Edinger-Westphal nuclei. Brain Structure and Function. 2016; 221:4073–4089. [PubMed: 26615603]

Mayr R. Structure and distribution of fibre types in the external eye muscles of the rat. Tissue Cell. 1971; 3:433–462. [PubMed: 18631565]

Mayr R, Gottschall J, Gruber H, Neuhuber W. Internal structure of cat extraocular muscle. Anatomy and Embryology (Berl). 1975; 148:25–34.

Mays LE. Neural control of vergence eye movements: Convergence and divergence neurons in midbrain. Journal of Neurophysiology. 1984; 51:1091–1108. [PubMed: 6726313]

Mays LE, Porter JD, Gamlin PD, Tello CA. Neural control of vergence eye movements: Neurons encoding vergence velocity. Journal of Neurophysiology. 1986; 56:1007–1021. [PubMed: 3783225]

Miller JM, Davison RC, Gamlin PD. Motor nucleus activity fails to predict extraocular muscle forces in oculomotor convergence. Journal of Neurophysiology. 2011; 105:2863–73. [PubMed: 21451064]

Morgan DL, Proske U. Vertebrate slow muscle: Its structure, pattern of innervation, and mechanical properties. Physiological Review. 1984; 64:103–169.

Morgan MW. Accommodation and vergence. American Journal of Optometry and Archives of American Academy of Optometry. 1968; 45:417–454. [PubMed: 4875838]

Moschovakis AK, Karabelas AB, Highstein SM. Structure-function relationships in the primate superior colliculus. II. Morphological identity of presaccadic neurons. Journal of Neurophysiology. 1988; 60:263–302. [PubMed: 3404220]

Namba T, Nakamura T, Grob D. Motor nerve endings in human extraocular muscle. Neurology. 1968a; 18:403–407. [PubMed: 4173449]

Namba T, Nakamura T, Takahashi A, Grob D. Motor nerve endings in extraocular muscles. Journal of Comparative Neurology. 1968b; 134:385–396. [PubMed: 4976421]

Nelson JS, Goldberg SJ, McClung JR. Motoneuron electrophysiological and muscle contractile properties of superior oblique motor units in cat. Journal of Neurophysiology. 1986; 55:715–726. [PubMed: 3701403]

Otero-Millan J, Macknik SL, Martinez-Conde S. Fixational eye movements and binocular vision. Frontiers in Integrative Neuroscience. 2014; 8:52. [PubMed: 25071480]

Pathmanathan JS, Cromer JA, Cullen KE, Waitzman DM. Temporal characterstics of neurons in the central mesencephalic redticular formation (cMRF) of head-unrestrained monkeys. Experimental Brain Research. 2006a; 168:471–492. [PubMed: 16292574]

Pathmanathan JS, Presnell R, Cromer JA, Cullen KE, Waitzman DM. Spatial characterstics of neurons in the central mesencephalic redticular formation (cMRF) of head-unrestrained monkeys. Experimental Brain Research. 2006b; 168:455–470. [PubMed: 16292575]

Perkins E, May PJ, Warren S. Feed-forward and feedback projections of midbrain reticular formation neurons in the cat. Frontiers in Neuroanatomy. 2014; 7:55. [PubMed: 24454280]

Perkins E, Warren S, May PJ. The mesencephalic reticular formation as a conduit for primate collicular gaze control: Tectal inputs to neurons targeting the spinal cord and medulla. The Anatomical Record (Hoboken). 2009; 292:1162–1181.

Porter JD, Guthrie BL, Sparks DL. Innervation of monkey extraocular muscles: Localization of sensory and motor neurons by retrograde transport of horseradish peroxidase. Journal of Comparative Neurology. 1983; 218:208–219. [PubMed: 6604075]

Robinson FR, Phillips JO, Fuchs AF. Coordination of gaze shifts in primates: Brainstem inputs to neck and extraocular motoneuron pools. Journal of Comparative Neurology. 1994; 346:43–62. [PubMed: 7962711]

Ruskell GL. The fine structure of innervated myotendinous cylinders in extraocular muscles of rhesus monkeys. Journal of Neurocytology. 1978; 7:693–708. [PubMed: 104011]

Ruskell GL, Kjellevold Haugen IB, Bruenech JR, van der Werf F. Double insertions of extraocular rectus muscles in humans and the pulley theory. Journal of Anatomy. 2005; 206:295–306. [PubMed: 15733302]

Schiaffino S, Reggiani C. Fiber types in mammalian skeletal muscles. Physiological Review. 2011; 91:1447–1531.

Schiller PH. The discharge characteristics of single units in the oculomotor and abducens nuclei of the unanesthetized monkey. Experimental Brain Research. 1970; 10:347–362. [PubMed: 4987208]

Spencer RF, Porter JD. Innervation and structure of extra-ocular muscles in the monkey in comparison to those of the cat. Journal of Comparative Neurology. 1981; 198:649–665. [PubMed: 7251934]

Spencer RF, Porter JD. Biological organization of the extra-ocular muscles. Progress in Brain Research. 2006; 151:43–80. [PubMed: 16221585]

Steinbach MJ. Proprioceptive knowledge of eye position. Vision Research. 1987; 27:1737–1744. [PubMed: 3328405]

Szabo J, Cowan WM. A stereotaxic atlas of the brain of the cynomolgus monkey (Macaca fascicularis). Journal of Comparative Neurology. 1984; 222:265–300. [PubMed: 6365984]

Tang X, Büttner-Ennever JA, Mustari MJ, Horn AK. Internal organization of medial rectus and inferior rectus muscle neurons in the C group of the oculomotor nucleus in monkey. Journal of Comparative Neurology. 2015; 523:1809–1823. [PubMed: 25684641]

Taylor RG, Abresch RT, Lieberman JS, Fowler WM Jr, Port-wood MM. Effect of pentobarbital on contractility of mouse skeletal muscle. Experimental Neurology. 1984; 83:254–263. [PubMed: 6692866]

Ugolini G, Klam F, Doldan DM, Dubayle D, Brandi AM, Büttner-Ennever JA, Graf W. Horizontal eye movement networks in primates as revealed by retrograde transneuronal transfer of rabies virus: Differences in monosynaptic input to “slow” and “fast” abducens motoneurons. Journal of Comparative Neurology. 2006; 498:762–785. [PubMed: 16927266]

Van Horn MR, Cullen KS. Dynamic characterization of agonist and antagonist oculomotor neurons during conjugate and disconjugate eye movements. Journal of Neurophysiology. 2009; 102:28–40. [PubMed: 19403746]

Waitzman DM, Silakov VL, Cohen B. Central mesencephalic reticular formation (cMRF) neurons discharging before and during eye movements. Journal of Neurophysiology. 1996; 75:1546–1572. [PubMed: 8727396]

Waitzman DM, Silakov VL, DePalma-Bowles S, Ayers AS. Effects of reversible inactivation of the primate mesencephalic reticular formation. I. Hypermetric goal-directed saccades. Journal of Neurophysiology. 2000a; 83:2260–2284. [PubMed: 10758133]

Waitzman DM, Silakov VL, DePalma-Bowles S, Ayers AS. Effects of reversible inactivation of the primate mesencephalic reticular formation. II. Hypometric vertical saccades. Journal of Neurophysiology. 2000b; 83:2285–2299. [PubMed: 10758134]

Waitzman DM, Van Horn MR, Cullen KE. Neuronal evidence for individual eye control in the primate cMRF. Progress in Brain Research. 2008; 171:143–150. [PubMed: 18718293]

Wang N, Perkins E, Zhou L, Warren S, May PJ. Anatomical evidence that the superior colliculus controls saccades through central mesencephalic reticular formation gating of omnipause neuron activity. Journal of Neuroscience. 2013; 33:16285–16296. [PubMed: 24107960]

Warren S, Waitzman DM, May PJ. Anatomical evidence for interconnections between the central mesencephalic reticular formation and cervical spinal cord in the cat and macaque. The Anatomical Record (Hoboken). 2008; 291:141–160.

Wasicky R, Horn AK, Büttner-Ennever JA. Twitch and nontwitch motoneuron subgroups in the oculomotor nucleus of monkeys receive different afferent projections. Journal of Comparative Neurology. 2004; 479:117–129. [PubMed: 15452829]

Wasicky R, Ziya-Ghazvini F, Blumer R, Lukas JR, Mayr R. Muscle fiber types of human extraocular muscles: a histochemical and immunohistochemical study. Investigative Ophthalmology & Visual Science. 2000; 41:980–990. [PubMed: 10752931]

Weir CR, Knox PC, Dutton GN. Does extraocular muscle proprioception influence oculomotor control? British Journal of Ophthalmology. 2000; 84:1071–1074. [PubMed: 10966971]

Wouterlood FG, Groenewegen HJ. Neuroanatomical tracing by use of *Phaseolus vulgaris*-leucoagglutinin (PHA-L): Electron microscopy of PHA-L-filled neuronal somata, dendrites, axons and axon terminals. Brain Research. 1985; 326:188–191. [PubMed: 3882193]

Zhang Y, Mays LE, Gamlin PD. Characteristics of near response cells projecting to the oculomotor nucleus. Journal of Neurophysiology. 1992; 67:944–960. [PubMed: 1588393]

Zhou L, Warren S, May PJ. The feedback circuit connecting the central mesencephalic reticular formation and the superior colliculus in the macaque monkey: Tectal connections. Experimental Brain Research. 2008; 189:485–496. [PubMed: 18553075]

Zimmermann L, May PJ, Pastor AM, Streicher J, Blumer R. Evidence that the extraocular motor nuclei innervate monkey palisade endings. Neuroscience Letters. 2011; 489:89–93. [PubMed: 21138754]

Zimmermann L, Morado-Diaz CJ, Davis-Lopez de Carrizosa MA, de la Cruz RR, May PJ, Streicher J, … Blumer R. Axons giving rise to the palisade endings of feline extraocular muscles display motor features. Journal of Neuroscience. 2013; 33:2784–2793. [PubMed: 23407938]

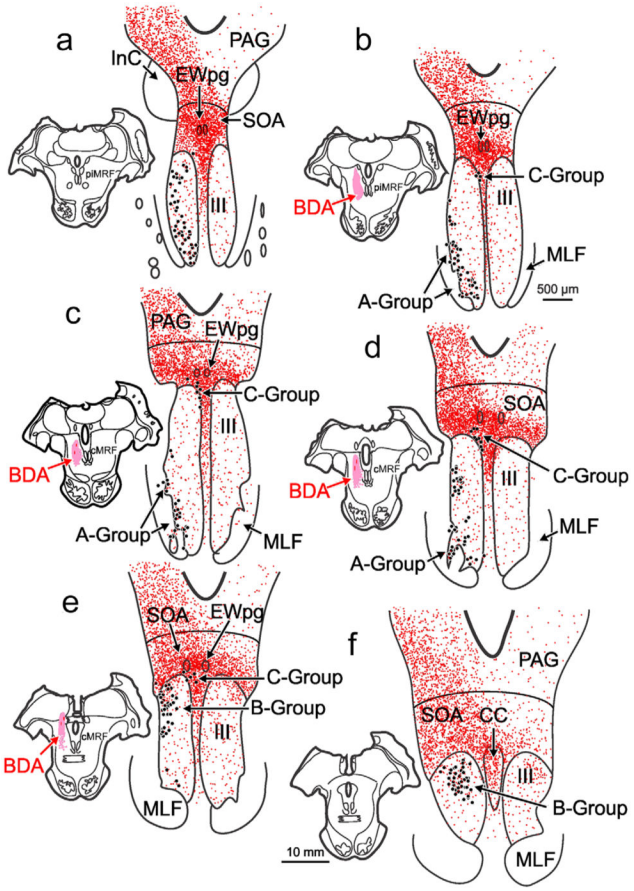

FIGURE 1.

Distribution of biotinylated dextran amine (BDA) labeled reticulo-oculomotor terminals with respect to medial rectus motoneurons found in the ipsilateral A-, B-, and C- groups. Chartings of a rostral to caudal series (**a**–**f**) of representative sections through the oculomotor nucleus (III) following a large, medial BDA injection centered in the left central mesencephalic reticular formation (cMRF) (insets **b**–**e**) that was combined with a choleratoxin subunit B conjugated to horseradish peroxidase (ChTB-HRP) injection into the left medial rectus muscle. This large injection resulted in dense axon terminal labeling (stipple) ipsilaterally within periaqueductal gray (PAG), bilaterally within the supraoculomotor area (SOA), and bilaterally, to a lesser extent, within III. Retrogradely labeled medial rectus motoneurons (dots) were located in the left A-, B-, and C-groups. There was extensive overlap between labeled cMRF terminals and labeled cells in the C-group (**b**–**e**). Terminals could also be observed within the regions containing medial rectus A-group (**a**–**d**) and B-group motoneurons (**d**–**f**) [Color figure can be viewed at wileyonlinelibrary.com]

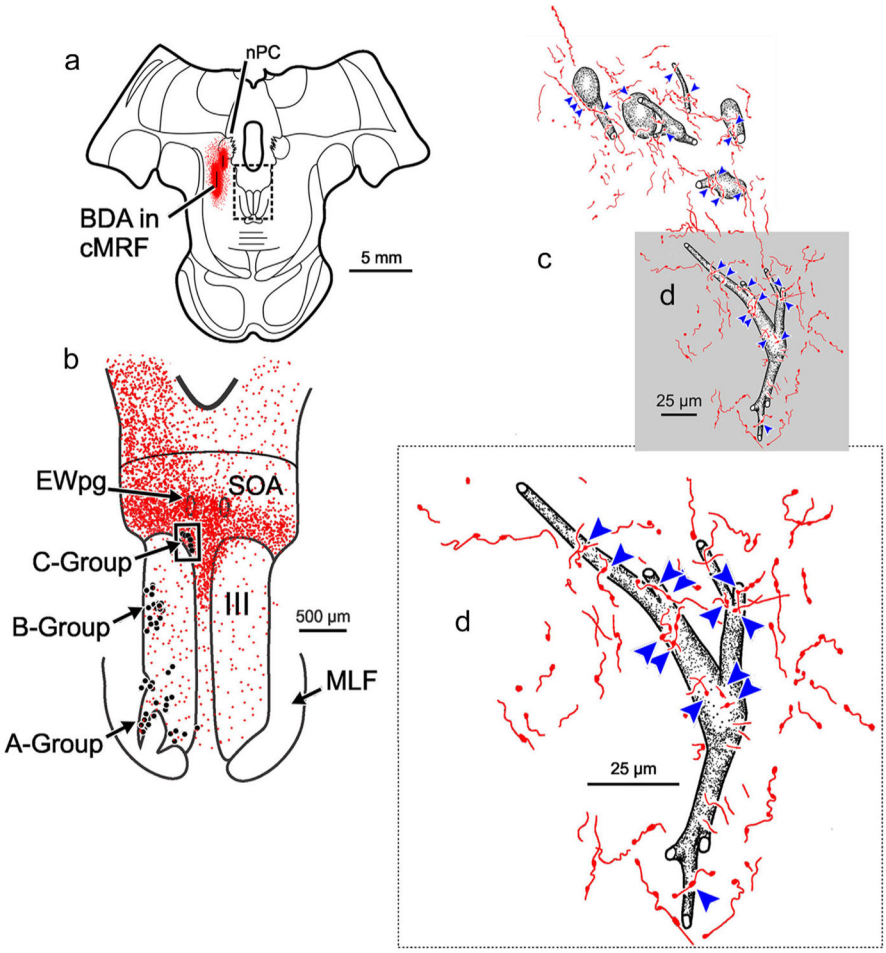

FIGURE 2.

BDA labeled reticulo-oculomotor terminals in close association with ipsilateral medial rectus C-group motoneurons. (**a**) Shows the section illustrated, demonstrating a portion of the injection of BDA (see Figure 1 for details) (Box in **a** indicates sample in **b**.) (**b**) Distribution of labeled cMRF axon terminals (stipple) in the SOA and III. The location of the ChTB-HRP labeled medial rectus motoneurons in the A-, B-, and C-groups is indicated by dots. (Box indicates sample **c**) (**c**). Numerous close associations (arrowheads) could be observed between cMRF axon terminals and every ipsilateral medial rectus C-group motoneuron. Gray box indicates area where the higher magnification insert **d** is from. Note the large number of close associations on the somata and proximal dendrites. [Color figure can be viewed at wileyonlinelibrary.com]

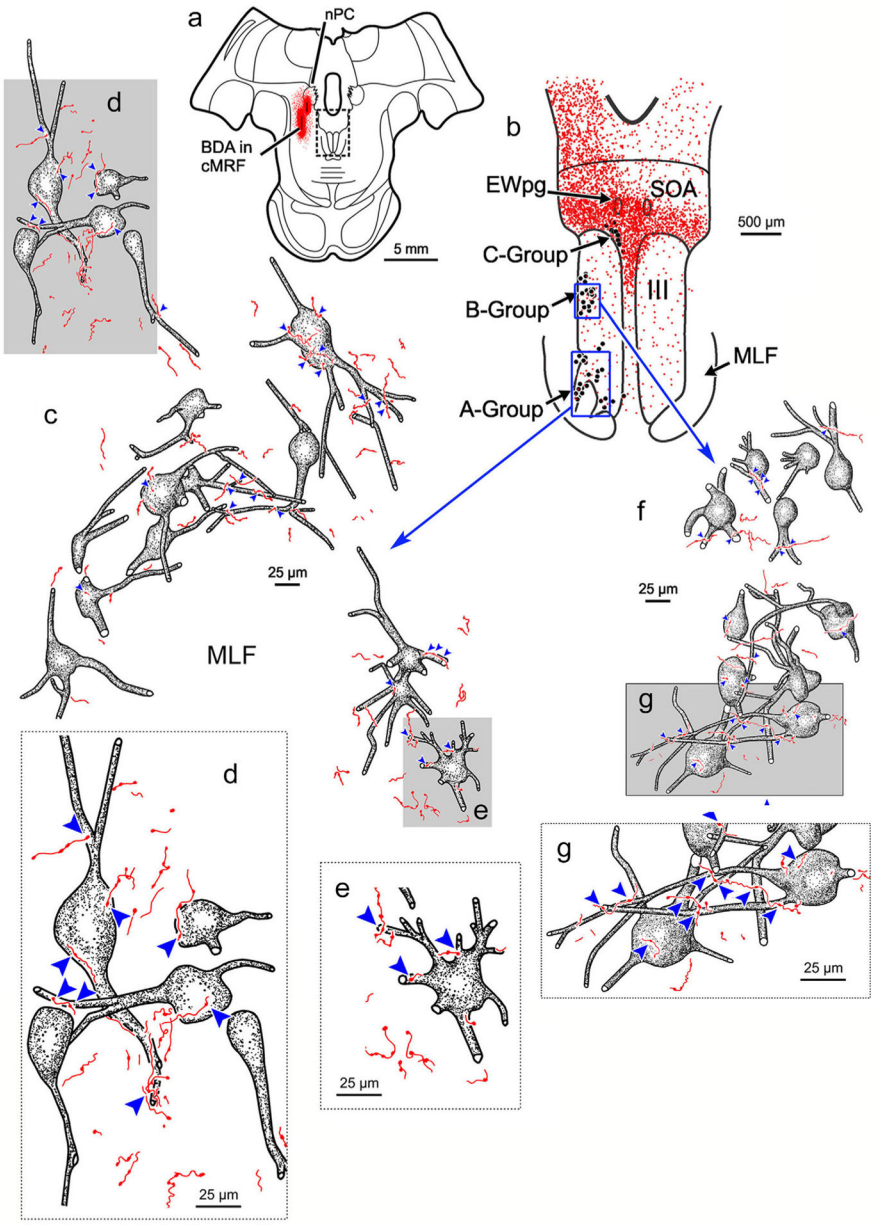

FIGURE 3.

BDA labeled reticulo-oculomotor terminals in close association with ipsilateral medial rectus A-group (**c**–**e**) and B-group (**f** and **g**) motoneurons. (**a**) Shows the section illustrated (Box in **a** indicates sample in **b**). In (**b**), labeled terminals (stipple) are distributed around and in III. ChTB-HRP labeled medial rectus motoneurons in the A-, B-, and C-groups are indicated by dots. (Boxes in **b** show sample areas for **c** and **f**.) (**c,f**) High magnification drawing of the retrogradely labeled medial rectus A-group and B-group motoneurons, respectively, showing close associations (arrowheads) with labeled cMRF terminals on many, but not all cells following a large injection of the cMRF. Gray boxes show location of high magnification insets shown in **d, e**, and **g**. [Color figure can be viewed at wileyonlinelibrary.com]

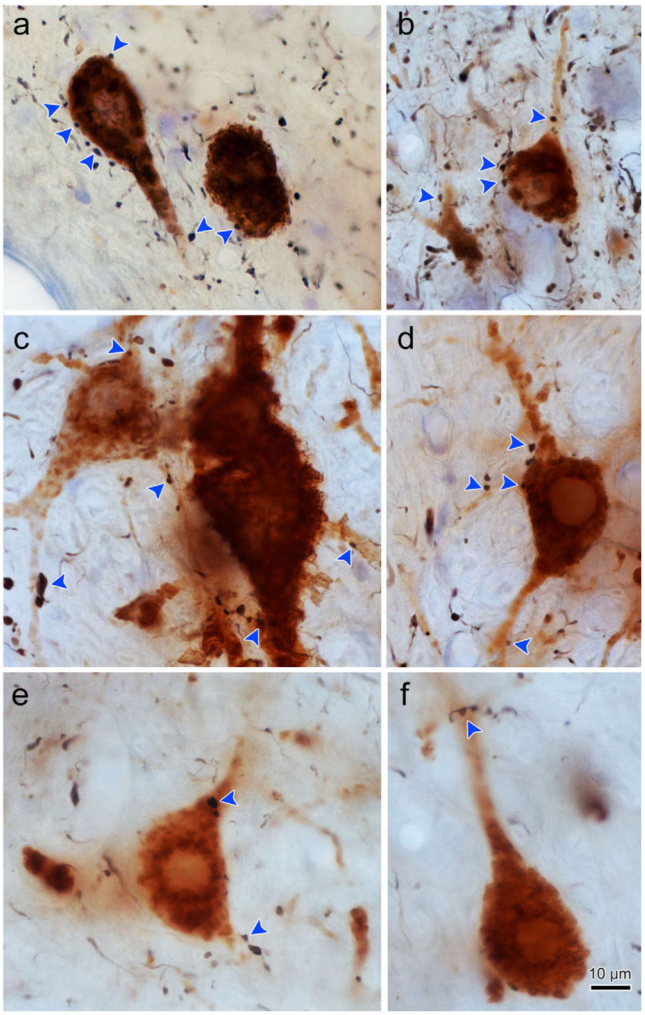

FIGURE 4.

Photomicrographs of BDA labeled cMRF axon terminals in close association with ipsilateral ChTB-HRP labeled medial rectus motoneurons. Plates **a** and **b** show C-group medial rectus MIF motoneurons with close associations (arrowheads) from cMRF boutons. Note the presence of several close associations on the cell bodies and dendrites. Plates **c** and **d** show A-group medial rectus motoneurons with axodendritic and axosomatic close associations. Plates **e** and **f** show B-group medial rectus motoneurons with primarily axodendritic close associations. Note the greater density of the terminals in the C-group region (**a** and **b**) compared to the A- and B-group regions (**c**–**f**). [1.0 micron thick *Z* planes merged to produce image: *a* =3, *b* =6, *c* =7, *d* =3, *e* =1, *f* =1]. [Color figure can be viewed at wileyonlinelibrary.com]

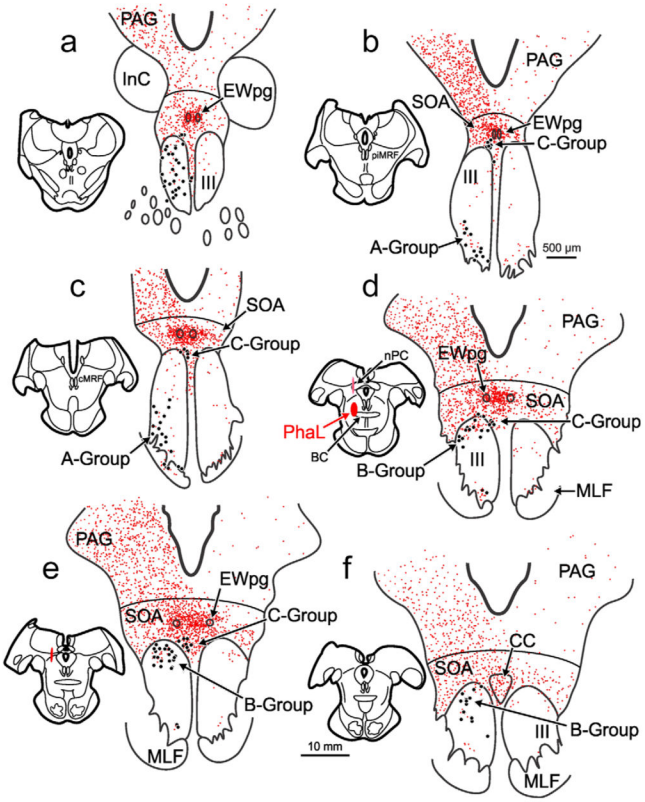

FIGURE 5.

Distribution of *Phaseolus vulgaris* leucoagglutinin (PhaL) labeled reticulo-oculomotor terminals with respect to medial rectus motoneurons found in the ipsilateral A-, B-, and C-groups. Chartings of a rostral to caudal series of representative sections through III following a medium-sized PhaL injection centered in the left cMRF (insets **d**–**e**) that was combined with a ChTB-HRP injection into the left medial rectus muscle. The cMRF injection site was well confined within the rostrocaudal extent of the nucleus (**d**). This injection resulted in axon terminal labeling (stipple) that could be observed ipsilaterally within the PAG, bilaterally within the SOA, and bilaterally, to a lesser extent, within III. Retrogradely labeled medial rectus motoneurons (dots) were located in the A-, B-, and C-groups. There was extensive overlap between labeled cMRF terminals and labeled cells in the C-group (**b**–**e**). Terminals could also be observed within the regions containing the A-group (**a**–**d**) and B-group (**d**–**f**) motoneurons. [Color figure can be viewed at wileyonlinelibrary.com]

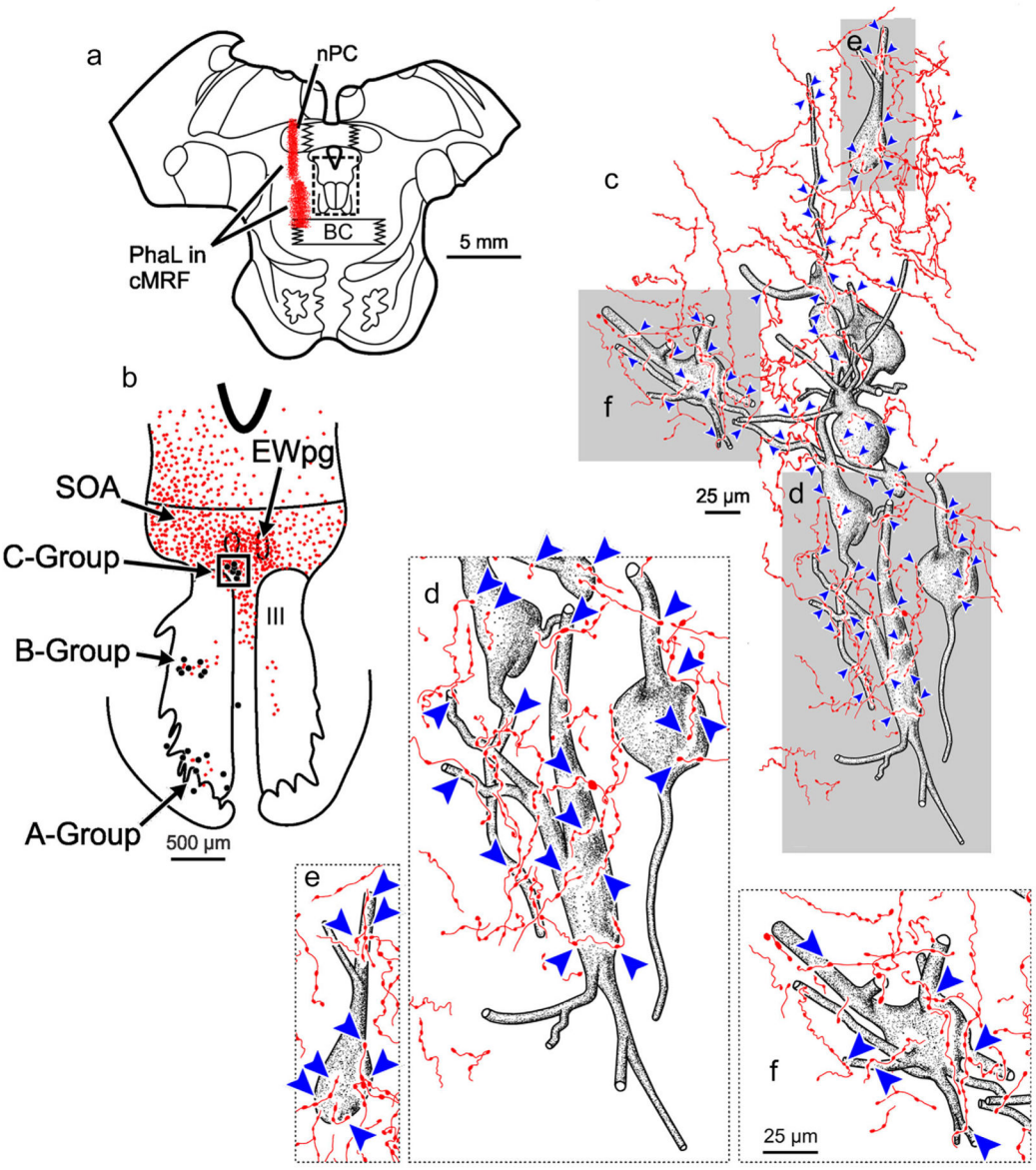

FIGURE 6.

PhaL labeled reticulo-oculomotor terminals in close association with ipsilateral medial rectus C-group motoneurons. (**a**) Shows the section illustrated and a portion of the PhaL injection site (Box shows sample in **b**.) (**b**) Distribution of labeled cMRF axon terminals (stipple) in the SOA. The location of the ChTB-HRP labeled medial rectus motoneurons in the A-, B-, and C-groups is indicated by dots. (Box shows sample in **c**.) (**c**) Numerous close associations (arrowheads) could be observed between cMRF axon terminals and every ipsilateral medial rectus C-group motoneuron seen. Gray boxes indicate areas where the higher magnification inserts **d**–**f** are taken from. [Color figure can be viewed at wileyonlinelibrary.com]

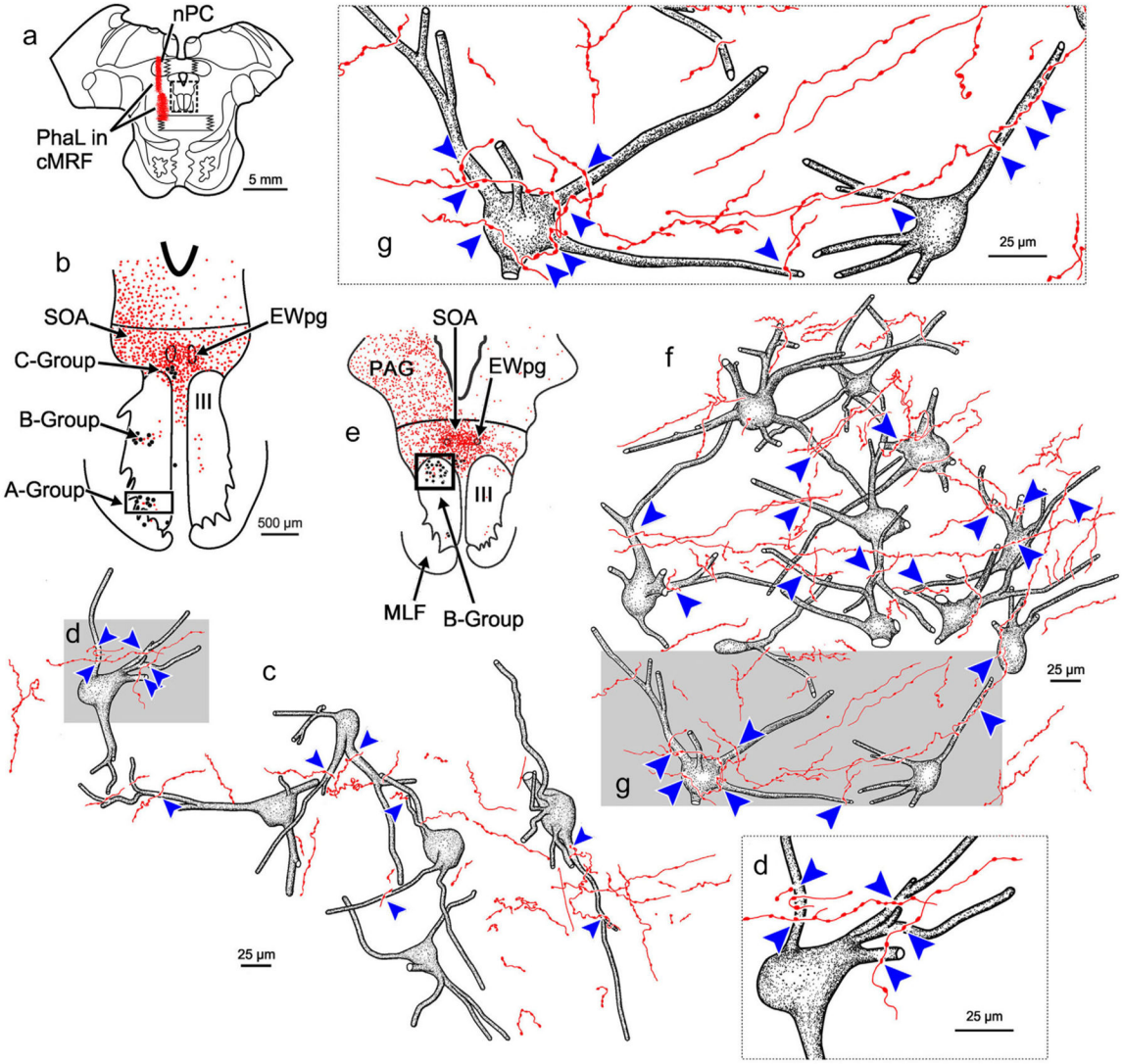

FIGURE 7.

PhaL labeled reticulo-oculomotor terminals in close association with ipsilateral medial rectus A-group motoneurons (**b**–**d**) and B-group motoneurons (**e**–**g**). (**a**) Shows the section illustrated. (Box shows region sampled in **b and e**.) (**b and e**) Distribution of anterogradely labeled cMRF axon terminals (stipple) and location of the ChTB-HRP labeled motoneurons (dots). (Boxes indicates areas sampled in **c and f**.) Several close associations (arrowheads) could be observed between cMRF axon terminals and some, but not all, A-group motoneurons (**c**) and most B-group motoneurons (**f**). Gray boxes indicate areas where the higher magnification inserts **d** and **g** are taken from. [Color figure can be viewed at wileyonlinelibrary.com]

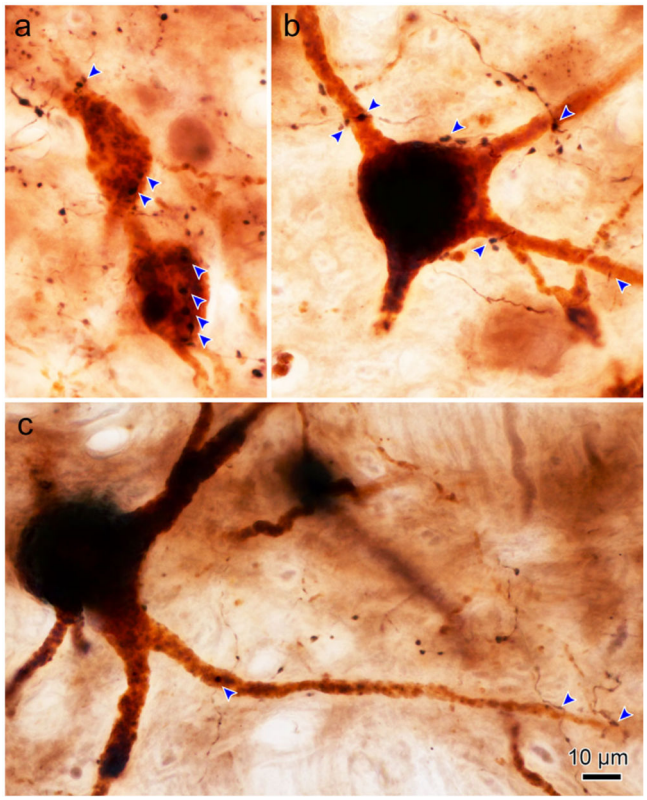

FIGURE 8.

Photomicrographs of PhaL labeled cMRF axon terminals in close association with ipsilateral medial rectus motoneurons labeled with ChTB-HRP. (**a**) Two C-group medial rectus MIF motoneurons with numerous axosomatic and axodendritic close associations. (**b**) A, B-group medial rectus motoneuron with axodendritic and axosomatic close associations. (**c**) An A-group medial rectus motoneuron with close associations. [1.0 micron thick *Z* planes merged to produce image: A =8, B =11, C =10]. [Color figure can be viewed at wileyonlinelibrary.com]

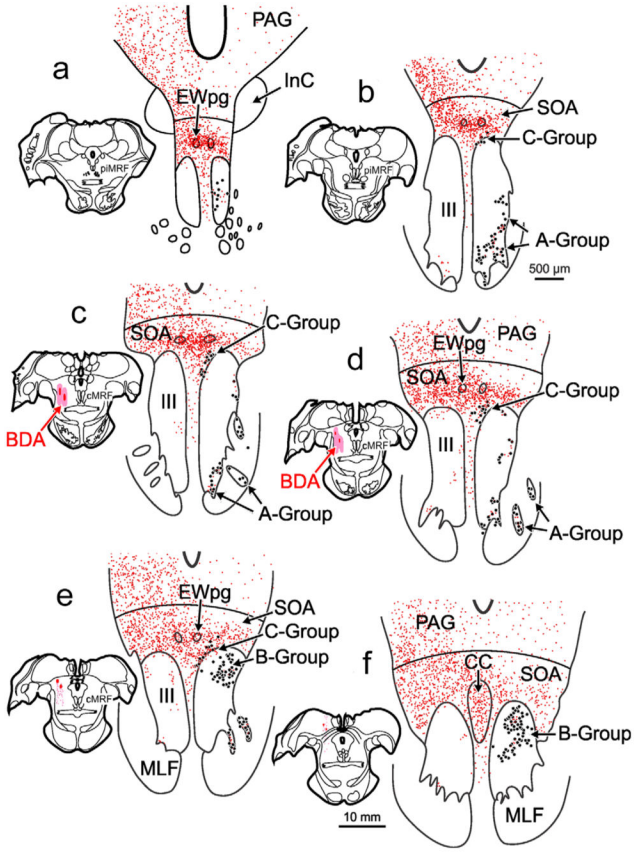

FIGURE 9.

Distribution of BDA labeled reticulo-oculomotor terminals with respect to medial rectus motoneurons found in the contralateral A-, B-, and C- groups. Chartings show a rostral to caudal series of representative sections (**a**–**f**) through III following a laterally located, BDA injection in the left cMRF (insets **c** and **d**) that was combined with ChTB-HRP injection into the right medial rectus muscle. The injection resulted in moderate axon terminal labeling (stipple) located ipsilaterally within the PAG and bilaterally within the SOA. A few terminals were present within III. ChTB-HRP labeled medial rectus motoneurons (dots) were located in the A-, B-, and C-groups. There was extensive overlap between labeled cMRF terminals in the SOA and the labeled cells in the contralateral C-group (**b**–**e**). Within contralateral III, terminal fields were minimal, with only a few terminals observed within the regions association with the right medial rectus A-group (**b**–**e**) and B-group (**e,f**). [Color figure can be viewed at wileyonlinelibrary.com]

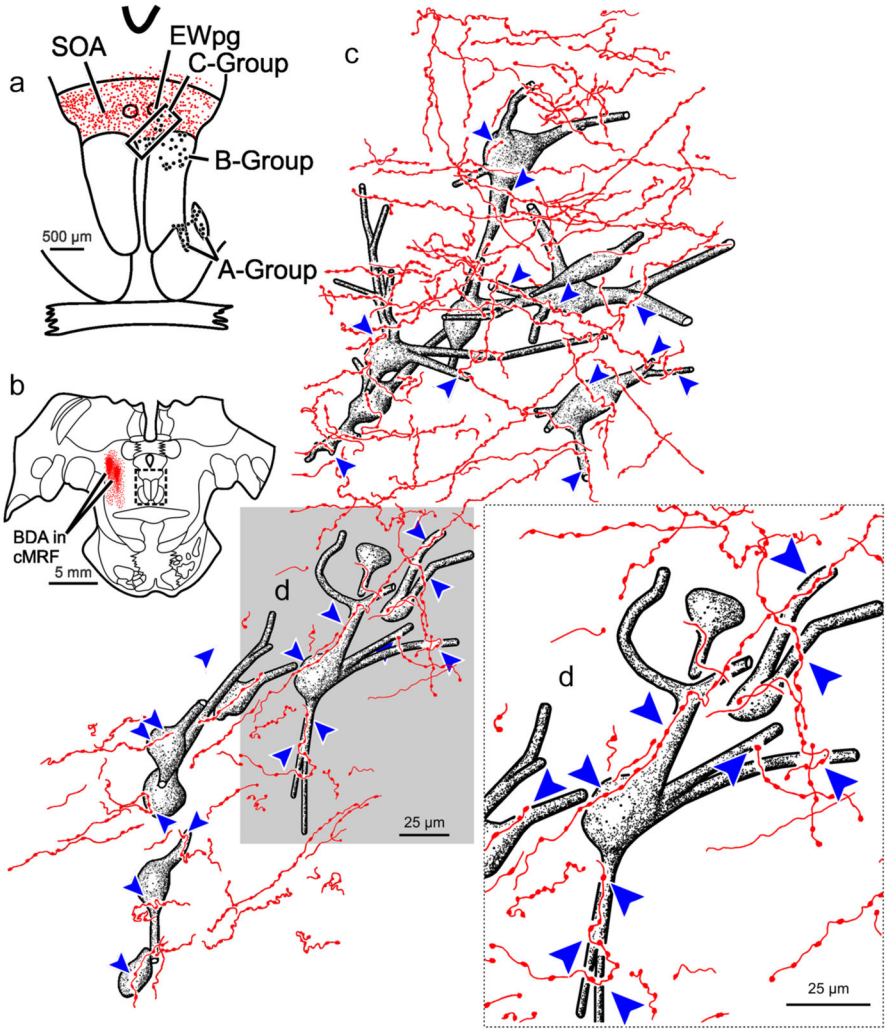

FIGURE 10.

BDA labeled reticulo-oculomotor terminals in close association with contralateral medial rectus C-group motoneurons. (**b**) Shows the section illustrated and a portion of the BDA injection site (see Figure 9 for details) (Box shows sample in **a**.) (**a**) The distribution of labeled cMRF axon terminals (stipple) and location of the A-, B-, and C-group medial rectus motoneurons (dots) are shown. (Box indicates region illustrated in **c**.) (**c**) Numerous close associations (arrowheads) can be observed between cMRF axon terminals and each of the contralateral medial rectus C-group motoneurons. Gray box indicates area where the higher magnification insert (**d**) is taken from. [Color figure can be viewed at wileyonlinelibrary.com]

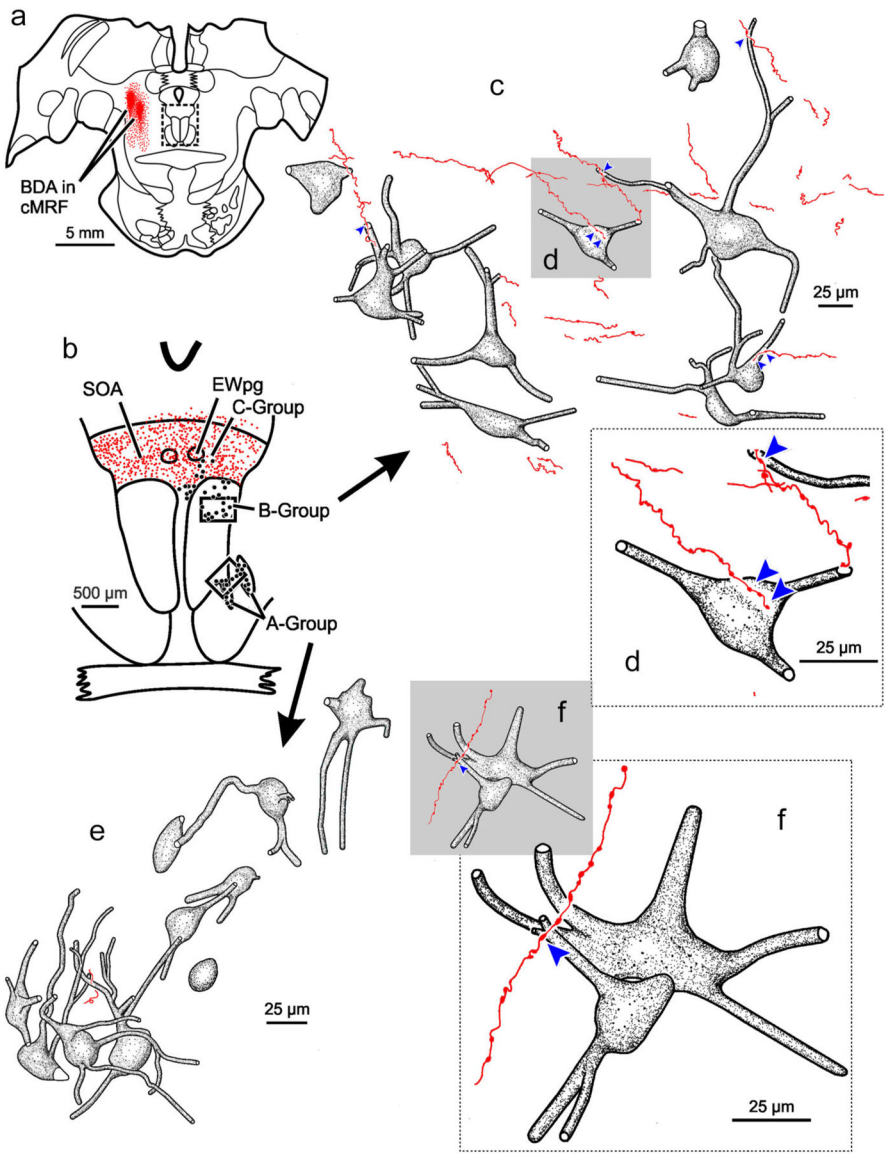

FIGURE 11.

BDA labeled reticulo-oculomotor terminals in close association with contralateral medial rectus A- and B-group motoneurons. (**a**) Shows the section illustrated and a portion of the BDA injection site (see Figure 9 for details) (Box shows sample in **b**.) (**b**) The distribution of labeled cMRF axon terminals (stipple) and location of the A-, B-, and C-group medial rectus motoneurons (dots) are shown. (Boxes indicate regions illustrated in **c** and **e**.) (**c** and **d**) Close associations (arrowheads) were observed between cMRF axon terminals and a few of the contralateral B-group medial rectus motoneurons. Gray box in **c** indicates area where the higher magnification insert in (**d**) is from. (**e** and **f**) A close association (arrowhead) observed between a cMRF axon terminal and only one of the contralateral A-group medial rectus motoneurons. Gray box in (**e**) indicates the area where the higher magnification insert shown (**f**) is from. [Color figure can be viewed at wileyonlinelibrary.com]

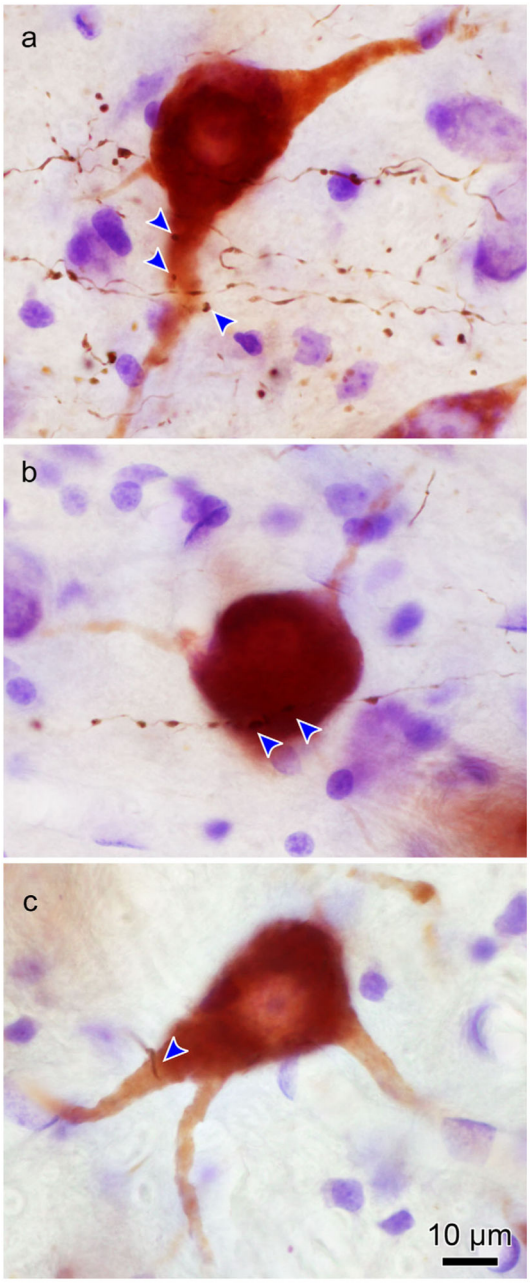

FIGURE 12.

Photomicrographs of the relationship between BDA labeled cMRF axon terminals and contralateral, ChTB-HRP labeled motoneurons. (**a**) A-, C-group medial rectus MIF motoneuron that has numerous axosomatic and axodendritic close associations (arrowheads) with cMRF boutons. (**b**) A-, B-group medial rectus motoneuron with a single axon displaying axosomatic close associations as it passes. (**c**) An example of an A-group motoneuron. Only one labeled axon is present in the field and it does not contact this cell. [1.0 micron thick *Z* planes merged to produce image: *a* =5, *b* =7, *c* =5]. [Color figure can be viewed at wileyonlinelibrary.com]

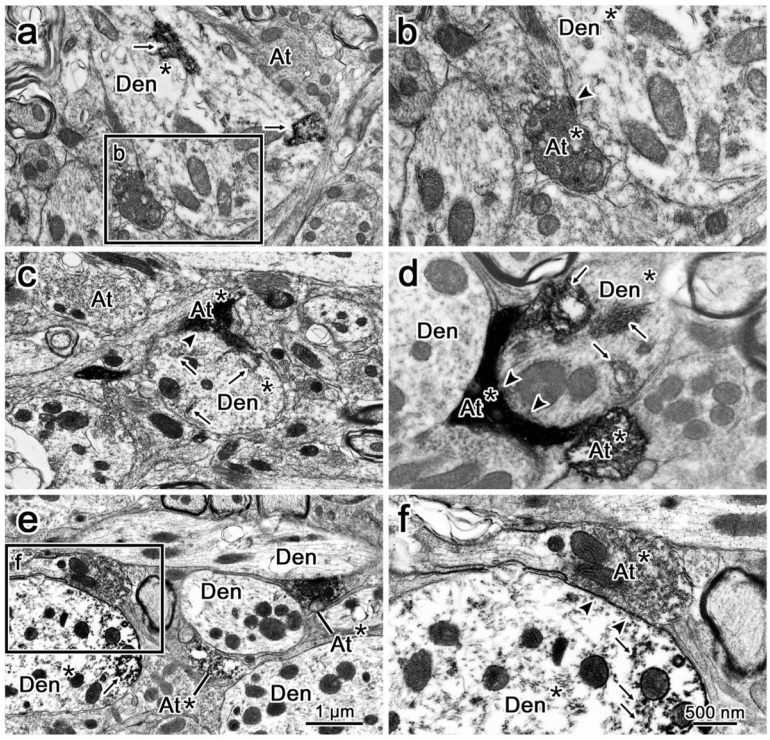

FIGURE 13.

Central mesencephalic reticular formation (cMRF) inputs synaptically contact medial rectus motoneurons. Electron micrographs show anterogradely labeled cMRF terminals in synaptic contact (arrowhead) with retrogradely labeled medial rectus motoneurons. (**a and c**) Low magnification views showing examples of a retrogradely labeled dendrites (Den*) from medial rectus C-group motoneurons ipsilateral (**a**) and contralateral (**c**) to the cMRF injection site. There is flocculent electron dense HRP reaction product (arrow) in the dendrites. Anterogradely labeled axon terminals (At*) from the BDA injection into the cMRF are more electron dense than an unlabeled axon terminals (At). (Boxed area in **a** is shown in **b**.) (**b**) A higher magnification view, shows the synaptic contact of an anterogradely labeled cMRF terminal (At*) onto the labeled dendrite (Den*). (**d**) An example of a retrogradely labeled B-group medial rectus dendrite (Den*) with an anterogradely labeled cMRF axon forming a synaptic contact (At*) onto it. There is also a second labeled cMRF axon terminal in close apposition to an unlabeled dendrite (Den). (**e**) A lower magnification view of labeled cMRF axon terminals in the region of the A-group medial rectus motoneurons. (Box in **e** shown at higher magnification in **f.) (f**) Retrogradely labeled A-group dendrite that receives a synaptic contact from a labeled cMRF terminal (At*). Scale bar in *a, c*, and *e* =1 um, in *b, d*, and *f* =500 nm

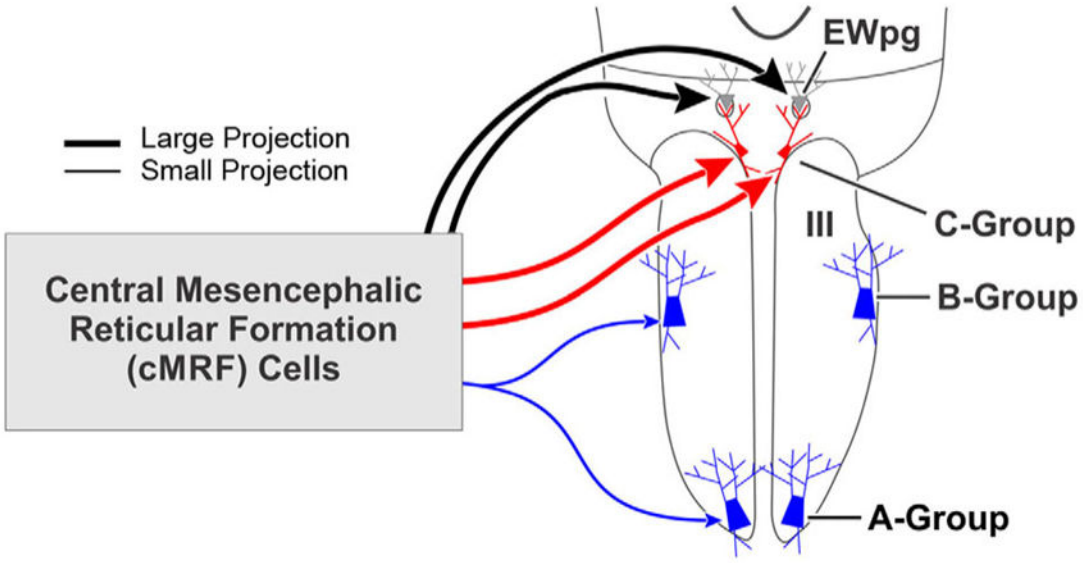

FIGURE 14.

Summary of cMRF connections to motoneuron types. The cMRF provides a large (thick line), bilateral projection to the medial rectus motoneurons in the C-group (present work) and to preganglionic motoneurons in the preganglionic Edinger-Westphal nucleus (EWpg) (May et al., 2016). In addition, there is a modest (thin line) projection to the medial rectus motoneurons within the ipsilateral A- and B-groups. Since the C-group contains motoneurons supplying multiply innervated fibers (MIFs), and the A- and B-groups contain motoneurons supplying singly innervated fibers (SIFs) the pattern of projections suggests the cMRF influences these two populations differently. [Color figure can be viewed at wileyonlinelibrary.com]